

A QUASI-OPTIMAL FACTORIZATION PRECONDITIONER FOR PERIODIC SCHRÖDINGER EIGENSTATES IN ANISOTROPICALLY EXPANDING DOMAINS*

BENJAMIN STAMM[†] AND LAMBERT THEISEN[‡]

Abstract. This paper provides a provably quasi-optimal preconditioning strategy of the linear Schrödinger eigenvalue problem with periodic potentials for a possibly non-uniform spatial expansion of the domain. The quasi-optimality is achieved by having the iterative eigenvalue algorithms converge in a constant number of iterations for different domain sizes. In the analysis, we derive an analytic factorization of the spectrum and asymptotically describe it using concepts from the homogenization theory. This decomposition allows us to express the eigenpair as an easy-to-calculate cell problem solution combined with an asymptotically vanishing remainder. We then prove that the easy-to-calculate limit eigenvalue can be used in a shift-and-invert preconditioning strategy to bound the number of eigensolver iterations uniformly. Several numerical examples illustrate the effectiveness of this quasi-optimal preconditioning strategy.

Key words. Periodic Schrödinger Equation, Iterative Eigenvalue Solvers, Preconditioner, Asymptotic Eigenvalue Analysis, Factorization Principle, Directional Homogenization

AMS subject classifications. 65N25, 65F15, 65N30, 35B27, 35B40

1. Introduction. This paper considers the spectral problem for linear time-independent Schrödinger-type operators. Let us consider a parametrized family of d -dimensional boxes Ω_L given by

$$(1.1) \quad \mathbf{z} \in \Omega_L = (0, L)^p \times (0, \ell)^q = \Omega_{\mathbf{x}} \times \Omega_{\mathbf{y}} \subset \mathbb{R}^d,$$

with coordinates $\mathbf{z} := (\mathbf{x}, \mathbf{y}) = (x_1, \dots, x_p, y_1, \dots, y_q)$ and dimensions $L, \ell \in \mathbb{R}$. Note that we provide an extension to arbitrary domains in [subsection 4.3](#) and only keep the box shape for the early chapters of the analysis. We denote by $H_0^1(\Omega_L)$ the standard Sobolev space of index 1 with zero Dirichlet trace on Ω_L .

Then we consider the eigenvalue problem: Find $(\phi_L, \lambda_L) \in (H_0^1(\Omega_L) \setminus \{0\}) \times \mathbb{R}$, such that

$$(1.2) \quad -\Delta\phi_L + V\phi_L = \lambda_L\phi_L \quad \text{in } \Omega_L.$$

Here, ϕ_L and λ_L are the eigenfunctions and -values, respectively, while the function V encodes an external potential applied to the system. Typically, we are interested in computing some of the smallest eigenpairs of [\(1.2\)](#).

For the analysis, we make the following assumptions about the potential:

- (A1) The potential V is directional-periodic with a period of 1 in each expanding direction: $V(\mathbf{x}, \mathbf{y}) = V(\mathbf{x} + \mathbf{i}, \mathbf{y}) \quad \forall (\mathbf{x}, \mathbf{y}) \in \Omega_L, \mathbf{i} \in \mathbb{Z}^p$;
- (A2) The potential V is essentially bounded: $V \in L^\infty(\Omega_L)$;
- (A3) The potential V is non-negative: $V \geq 0$ a.e. in Ω_L .

Note that under the assumption (A2), we can always apply a constant spectral shift to the potential without affecting the eigenfunctions to fulfill (A3). Of course,

*L^AT_EX compiled on May 25, 2022.

Funding: This work was supported by the German Research Foundation (DFG) under project 411724963.

[†] Applied and Computational Mathematics, RWTH Aachen University, 52062 Aachen, Germany (best@acom.rwth-aachen.de).

[‡] Corresponding author. Applied and Computational Mathematics, RWTH Aachen University, 52062 Aachen, Germany (theisen@acom.rwth-aachen.de).

(A1) is only chosen for simplicity and arbitrary periods are possible. Furthermore, we could extend the theory to general elliptic operators satisfying the properties of [subsection 2.1](#). [Figure 1a](#) presents the geometrical framework.

We focus on the case of q fixed dimensions of length ℓ . In contrast, the other p dimensions expand with $L \rightarrow \infty$. This geometric setup allows us to study chain-like ($d = 2, p = 1$) or plane-like ($d = 3, p = 2$) domains with $L \rightarrow \infty$. These are the most common application cases. However, the setup is not limited to $d \leq 3$, and all results also hold in the general case.

Suppose one aims to solve for the ground-state eigenpair (smallest eigenvalue). In that case, the convergence rate of typical numerical algorithms [[20](#), p53] depends on the fundamental ratio between the first and the second ($\lambda_L^{(1)} < \lambda_L^{(2)}$) eigenvalue

$$(1.3) \quad r_L := |\lambda_L^{(1)}|/|\lambda_L^{(2)}| < 1.$$

Our geometrical setup of Ω_L , with $(0, L)^p \rightarrow (0, \infty)^p$ and $(0, \ell)^q$ being fixed, can lead to a collapsing fundamental gap $\lambda_L^{(1)} - \lambda_L^{(2)} \rightarrow 0$ and thus $r_L \rightarrow 1$ as $L \rightarrow \infty$. This will deteriorate the convergence rate in the limit. Therefore, the eigensolver routine needs more and more iterations to converge to a fixed tolerance as L increases. To overcome this problem, we theoretically study the operator's spectrum in [\(1.2\)](#) to construct a suitable shift-and-invert preconditioner [[51](#), p193], such that the preconditioned fundamental gap $r_L(\sigma) := |\lambda_L^{(1)} - \sigma|/|\lambda_L^{(2)} - \sigma|$ is uniformly bounded above by a constant $C < 1$, for all $L > L^*$. For this strategy to work, we need to choose a shift σ based on the asymptotic behavior of the problem. As it turns out later, the quasi-optimal shift σ has to be the asymptotic eigenvalue $\lambda_\infty := \lim_{L \rightarrow \infty} \lambda_L^{(1)}$. Throughout this paper, we understand quasi-optimality in terms of eigensolver iterations, which belong to $\mathcal{O}(1)$ for all L . This complexity is optimal except for an L -independent multiplicative constant. Also, note that we follow [[51](#), p193] and understand preconditioning in the eigenvalue context as a mechanism to speed up the convergence of an iterative solver by applying a spectral transformation [[20](#), p43].

1.1. Motivation: Collapsing Fundamental Gap for the Laplace Eigenvalue Problem. Even for the simplest potential satisfying the assumptions (A1)–(A3), namely $V(\mathbf{z}) = 0$, the fundamental gap r_L decreases if only a subset of directions in Ω_L is increased. The simplicity of the Laplace eigenvalue problem allows us to highlight the main challenges by considering the explicitly known eigenvalues. For $p = 1$ and $q = 1$, the pure Laplace eigenvalue problem has eigenvalues $\lambda_L^{(1)} = \pi^2/L^2 + \pi^2/\ell^2, \lambda_L^{(2)} = 4\pi^2/L^2 + \pi^2/\ell^2$. It is then evident that $\lim_{L \rightarrow \infty} \lambda_L^{(1)}/\lambda_L^{(2)} = 1$ for $L \rightarrow \infty$. Thus, this leads to a decreasing converge rate r_L . The collapsing fundamental gap is visible in the eigenvalue lattice illustrated in [Figure 1b](#). In such a representation, each point represents an eigenvalue $\lambda_L^{(m)}$, and its distance to the origin corresponds to $\sqrt{\lambda_L^{(m)}/\pi}$. All eigenvalues will form continuous x -parallel lines for the asymptotic case of $L \rightarrow \infty$. For this Laplace eigenvalue problem, a shift of $\sigma = \lambda_\infty = \pi^2/\ell^2$ would lead to $\lim_{L \rightarrow \infty} r_L(\sigma) = 1/4 < 1$.

This simple example serves as a motivation. However, to give a systematic approach to choosing the asymptotic correct shift σ in the general case, we develop a framework for characterizing the asymptotic behavior of the spectral properties for Schrödinger operators with periodic potentials satisfying (A1)–(A3). Knowing the asymptotic behavior will allow solving the algebraic eigenvalue problem within only a constant number of eigensolver iterations.

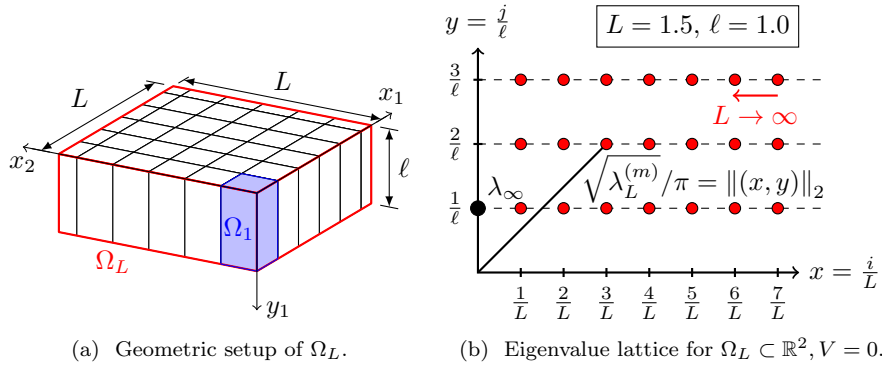


FIG. 1. *Figure 1a*: Geometric setup with $p = 2$ expanding directions with length $L = 5.5$ and $q = 1$ fixed dimensions with length $\ell = 2$. *Figure 1b*: The Dirichlet Laplacian spectrum on a rectangle domain $\Omega_L = (0, L) \times (0, \ell)$ mapped to an eigenvalue lattice.

1.2. State-of-the-Art and Context. We can embed our results into existing research for three different aspects – the considered model equation, the geometrical setup with the present periodic potential, and other mathematical analyses for related equations.

First, the Schrödinger equation (1.2) describes the stationary states of the wave function ϕ_L for a quantum-mechanical system influenced by an external potential V . Therefore, example applications naturally arise in computational chemistry and quantum mechanics. Since the present model is one of the simpler models, it is only suitable for the direct simulation of basic quantum systems. In more elaborate electronic structure calculations, a nonlinear version of the Schrödinger equation is used. However, there is always a need to solve systems similar to (1.2) in self-consistent field (SCF) iterations [41, 24, 44] or other iteration schemes to solve these nonlinear Schrödinger-type equations [15, 16, 17]. One of such examples is the Bose–Einstein condensate, either modeled with random or disorder potentials [14, 11] or modeled with the Gross–Pitaevskii eigenvalue problem [12, 13, 11, 42]. Other applications for the same equation (1.2) arise in studying the power distribution in a nuclear reactor core [5, 8, 38].

Second, when it comes to the geometric setup of only a subset of dimensions expanding, applications arise, for example, in material science to study the electronic properties of plane-like, layered [26, 25] or chain-like structures, such as carbon nanotubes [1] or polymers chains [59].

Third, from a mathematical point of view, the study of elliptic operators in the context of source [37, 36, 54, 34, 31, 28, 30] or eigenvalue problems [60, 23] with homogenization is closely related since V is periodic (at least directional in our setup). Also, for eigenvalue problems with periodic coefficients, results in [33, 29, 32] show the presence of an asymptotic limit when the domain expands in some directions to infinity. Finally, from a technical point of view, our analysis in section 2 extends aspects of the work by Allaire et al. in [6, 5, 9, 4, 8, 7]. Especially the concept of factorization will be one of the main techniques in our analysis. It allows us to analytically describe the spectrum of the system in terms of easier cell problems. This idea traces back to [57, 46, 47].

1.3. Contribution and Main Results. This work aims to provide a numerical framework to solve the eigenvalue problem (1.2) in a fixed number of eigensolver iterations for all domain sizes $L \rightarrow \infty$. We, therefore, propose a shift-and-invert strategy with a quasi-optimally chosen shift. The theoretical derivation of this particular shift is based on the following factorization of the eigenfunctions (see Theorem 2.5 for a more precise statement)

$$(1.4) \quad \phi_L^{(m)} = \psi \cdot u_{y,1} \cdot u_{y,2}^{(m)} = \varphi_y \cdot u_{y,2}^{(m)},$$

$$(1.5) \quad \lambda_L^{(m)} = \lambda_\psi + \lambda_{u_{y,1}} + \lambda_{u_{y,2}}^{(m)} = \lambda_{\varphi_y} + \lambda_{u_{y,2}}^{(m)} = \lambda_{\varphi_y} + \mathcal{O}(1/L^2).$$

The above characterization highlights that we can simply use λ_{φ_y} as the quasi-optimal shift since we will show that the remaining term $\lambda_{u_{y,2}}^{(m)}$ tends to zero as $L \rightarrow \infty$ for all m . The $\mathcal{O}(1/L^2)$ contribution in (1.5) is not uniform in m since it depends on the m -th eigenvalue of a homogenized equation, as shown later in Theorem 2.8. In contrast to existing literature, this statement considers the case where only a subset of dimensions expands, and the periodicity is directional, which is essential given the potential practical applications. The eigenpair $(\varphi_y, \lambda_{\varphi_y})$ can be obtained in a constant time since it does not depend on $L \rightarrow \infty$ as it is a solution to a fixed-size spectral cell problem. We then show that this eigenpair is the asymptotic limit as

$$(1.6) \quad \lim_{L \rightarrow \infty} \lambda_L^{(m)} = \lambda_{\varphi_y}.$$

These results, then, directly imply that the preconditioned fundamental ratio r_L is uniformly bounded from above by a constant for all $L > L^*$, which is smaller than one (see Theorem 2.9 for a more precise statement). Since the convergence speed of the iterative eigensolvers depends on precisely this ratio, they converge in a constant number of iterations, and our goal is achieved.

The main challenges arise in the analysis and the quasi-optimality proof of the preconditioner. Using factorization results to construct a quasi-optimal preconditioner for an anisotropic domain size increase, which can be computed in $\mathcal{O}(1)$, is not covered, up to our knowledge, in the existing literature. Moreover, although the idea of factorization is not new (see the references in subsection 1.2), it was not yet applied in the context of weighted and thus potentially degenerate Sobolev spaces. However, precisely this setup of degenerate weights is necessary for our quasi-optimality analysis since the zero Dirichlet boundary conditions on the \mathbf{y} -boundary significantly contribute to the asymptotic behavior of the spectrum. In addition, proving quasi-optimality also requires uniform bounds of the preconditioned system's fundamental ratio. Thus, another challenge is interpreting the expanding problem as a homogenization problem in a degenerate situation. This observation allows us to explicitly determine the asymptotic behavior of the m -dependent contribution in (1.4) and (1.5). However, unlike the classical homogenization theory, our homogenized limit is purely determined by an p - rather than an $(p+q)$ -dimensional problem, which seems to be a unique specialty of anisotropic expansion problems.

1.4. Outline. In section 2, we present the theoretical framework for the factorization approach in subsection 2.2, which allows us to consider the remaining simplified problems using the theory of homogenization in subsection 2.3 to derive quasi-optimality statements. We then discretize and solve the eigensystem in section 3 and show that the theoretical results also hold when specific subspace properties are met in the discrete setting. Next, section 4 presents various numerical examples and shows

the relevance of the method for solving practical problems. Finally, we conclude with some remarks and point out future work in [section 5](#).

2. Factorization and Homogenization of the Model Problem. This chapter will use factorization and homogenization to derive the asymptotic spectrum, which allows us to specify the limit eigenvalue $\lambda_{\varphi_y} = \lim_{L \rightarrow \infty} \lambda_L^{(m)}$.

2.1. Existence and Regularity Results. The second-order partial differential operator in (1.2) is self-adjoint (by the symmetry of the diffusion matrix δ_{ij}), is positive-definite (by ellipticity/coercivity of the Laplacian plus a non-negative potential), and has bounded coefficients (since $V \in L^\infty(\Omega_L)$). We can therefore recall the classical existence results from [40, 57, 42] to establish the well-posedness of our problem, that there exists a sequence $(m = 1, \dots, \infty)$ of eigenvalues with finite multiplicity $\lambda_L^{(m)}$ and a sequence of eigenfunctions $\phi_L^{(m)}$ (orthogonal basis of $H_0^1(\Omega_L)$) such that $0 < \lambda_L^{(1)} < \lambda_L^{(2)} \leq \lambda_L^{(3)} \leq \dots \rightarrow \infty$ and $\phi_L^{(1)} > 0$ a.e. in Ω_L .

2.2. Factorization of the Eigenfunctions and Eigenvalues. Our next step is to establish factorizations to solve the eigenvalue problem (1.2). Thus, we describe splitting an eigenfunction into a product of two or more functions and splitting an eigenvalue into the sum of two or more eigenvalues. This splitting can be seen as a generalization to the separation of variables for the pure Laplacian case.

Let $\mathcal{D}(\Omega_L) = C_c^\infty(\Omega_L)$ be the space of compactly supported test functions on Ω_L and ρ a weight function (measurable and positive a.e. in Ω_L). We then use the weighted Sobolev [48, 57] spaces as

$$(2.1) \quad H^1(\Omega_L; \rho) = \left\{ u \in \mathcal{D}'(\Omega_L) \mid \|u\|_{H^1(\Omega_L; \rho)} < \infty \right\},$$

$$(2.2) \quad H_{\mathcal{B}_x, \mathcal{B}_y}^1(\Omega_L; \rho) = \left\{ u \in H^1(\Omega_L; \rho) \mid \begin{cases} \mathcal{B}_x(u) = 0 \text{ on } \partial(0, L)^p \times (0, \ell)^q \\ \mathcal{B}_y(u) = 0 \text{ on } (0, L)^p \times \partial(0, \ell)^q \end{cases} \right\},$$

for some general boundary operators $\mathcal{B}_x, \mathcal{B}_y$, which are equipped with the weighted norm

$$(2.3) \quad \|\cdot\|_{H^1(\Omega_L; \rho)} = \sqrt{\|\nabla \cdot\|_{L^2(\Omega_L; \rho)}^2 + \|\cdot\|_{L^2(\Omega_L; \rho)}^2},$$

using $\|\cdot\|_{L^2(\Omega_L; \rho)}^2 := \|\sqrt{\rho} \cdot\|_{L^2(\Omega_L)}^2$ in the classical L^2 -sense. The corresponding scalar product is $\langle \cdot, \cdot \rangle_{L^2(\Omega_L; \rho)} = \langle \rho \cdot, \cdot \rangle_{L^2(\Omega_L)}$. For the boundary operators, we use $\mathcal{B}_x, \mathcal{B}_y \in \{\mathcal{B}_d, \mathcal{B}_n, \mathcal{B}_\#\}$ with

$$(2.4) \quad \text{Dirichlet: } \mathcal{B}_d(u)(\mathbf{z}) = u(\mathbf{z}),$$

$$(2.5) \quad \text{Neumann: } \mathcal{B}_n(u)(\mathbf{z}) = \rho(\mathbf{z}) \nabla u(\mathbf{z}) \cdot \mathbf{n}(\mathbf{z}),$$

$$(2.6) \quad \text{Periodic: } \mathcal{B}_\#(u)(\mathbf{z}) = u(\mathbf{z}) - u\left((z_i - n_i(\mathbf{z})L)_{i=1}^p, (z_i - n_i(\mathbf{z})\ell)_{i=p+1}^q\right),$$

where the unit normal-vector is denoted by $\mathbf{n}(\mathbf{z})$ for $\mathbf{z} \in \partial\Omega_L$.

In the following, we use multiple eigenvalue problems and their solutions. Therefore, we unify the notation and introduce the abstract notation:

DEFINITION 2.1 (Prototype of a Schrödinger eigenvalue problem). *For $\Omega_L = (0, L)^p \times (0, \ell)^q \subset \mathbb{R}^d$, $0 \leq \rho, V \in L^\infty(\Omega_L)$, and $1/\rho \in L_{\text{loc}}^1(\Omega_L)$, we define*

$$(2.7) \quad \left(u_{\mathcal{B}_x, \mathcal{B}_y, \rho, V}^{(m)}(\Omega_L), \lambda_{\mathcal{B}_x, \mathcal{B}_y, \rho, V}^{(m)}(\Omega_L) \right),$$

to be the m -th eigenpair (including multiplicities) of the generalized Schrödinger-type eigenvalue problem: Find $(u, \lambda) \in (H_{\mathcal{B}_x, \mathcal{B}_y}^1(\Omega_L; \rho) \setminus \{0\}) \times \mathbb{R}$, such that

$$(2.8) \quad -\nabla \cdot (\rho \nabla u) + Vu = \lambda \rho u \text{ in } \Omega_L.$$

Remark 2.2. If the weight ρ is zero only at the boundary of Ω_L , then we have $1/\rho \in L_{\text{loc}}^1(\Omega_L)$, which implies that $H_{\mathcal{B}_x, \mathcal{B}_y}^1(\Omega_L; \rho)$ is a Banach space [48, p235]. On the other hand, in the case of ρ being bounded from above and uniformly positive, i.e., $0 < c < \rho < C$ a.e. in Ω_L , the ρ -weighted Sobolev space from (2.1) is equivalent to the classical Sobolev space $H_{\mathcal{B}_x, \mathcal{B}_y}^1(\Omega_L; \rho) = H_{\mathcal{B}_x, \mathcal{B}_y}^1(\Omega_L)$, and we omit ρ in the notation.

Remark 2.3 (Weak form). The corresponding weak formulation of (2.8) reads: Find $(u, \lambda) \in (H_{\mathcal{B}_x, \mathcal{B}_y}^1(\Omega_L; \rho) \setminus \{0\}) \times \mathbb{R}$ such that

$$(2.9) \quad \forall v \in H_{\mathcal{B}_x, \mathcal{B}_y}^1(\Omega_L; \rho) : \int_{\Omega_L} \rho \nabla u \cdot \nabla v \, dz + \int_{\Omega_L} V u v \, dz = \lambda \int_{\Omega_L} \rho u v \, dz.$$

Remark 2.4 (Min-max characterization). Since the weight ρ is a scalar function, (2.8) is self-adjoint for the presented boundary conditions, and we can express the eigenpair through the min-max characterization (c.f. [46, 35]):

$$(2.10) \quad \lambda^{(m)} = \min_{\substack{W_m \subset H_{\mathcal{B}_x, \mathcal{B}_y}^1(\Omega_L; \rho) \\ \dim W_m = m}} \max_{\substack{u \in W_m \\ u \neq 0}} \mathcal{R}_{\rho, V}(u),$$

with the Rayleigh quotient, defined by

$$(2.11) \quad \mathcal{R}_{\rho, V}(u) = \frac{\int_{\Omega_L} \rho(z) \nabla u(z) \cdot \nabla u(z) \, dz + \int_{\Omega_L} V(z) u^2(z) \, dz}{\int_{\Omega_L} \rho(z) u^2(z) \, dz},$$

which is identical for all the considered boundary conditions $\mathcal{B}_x, \mathcal{B}_y \in \{\mathcal{B}_d, \mathcal{B}_n, \mathcal{B}_\#\}$ of Definition 2.1.

We define $E_x^\# : H_{\mathcal{B}_\#, \mathcal{B}_y}^1(\Omega_1; \rho) \rightarrow H_{\mathcal{B}_\#, \mathcal{B}_y}^1(\Omega_L; \rho)$ as the periodic extension operator in the x -direction for an x -periodic weight ρ and $\mathcal{B}_y \in \{\mathcal{B}_d, \mathcal{B}_n, \mathcal{B}_\#\}$. We are now prepared to state our first main theoretical result:

THEOREM 2.5 (Factorization of eigenfunctions and summation of eigenvalues).

The m -th eigenfunction of the Schrödinger eigenvalue problem (1.2) can be factorized into

$$(2.12) \quad u_{\mathcal{B}_d, \mathcal{B}_d, 1, V}^{(m)} = \psi \cdot u^{(m)} = \psi \cdot u_{x,1} \cdot u_{x,2}^{(m)} = \varphi_x \cdot u_{x,2}^{(m)}$$

$$(2.13) \quad = \psi \cdot u_{y,1} \cdot u_{y,2}^{(m)} = \varphi_y \cdot u_{y,2}^{(m)}$$

while the m -th eigenvalue can be summed correspondingly as

$$(2.14) \quad \lambda_{\mathcal{B}_d, \mathcal{B}_d, 1, V}^{(m)} = \lambda_\psi + \lambda_u^{(m)} = \lambda_\psi + \lambda_{u_{x,1}} + \lambda_{u_{x,2}}^{(m)} = \lambda_{\varphi_x} + \lambda_{u_{x,2}}^{(m)}$$

$$(2.15) \quad = \lambda_\psi + \lambda_{u_{y,1}} + \lambda_{u_{y,2}}^{(m)} = \lambda_{\varphi_y} + \lambda_{u_{y,2}}^{(m)}$$

where

$$(2.16) \quad \psi = E_x^\# u_{\mathcal{B}_\#, \mathcal{B}_\#, 1, V}^{(1)}(\Omega_1), \quad u^{(m)} = u_{\mathcal{B}_d, \mathcal{B}_d, \psi^2, 0}^{(m)}(\Omega_L),$$

$$(2.17) \quad u_{x,1} = u_{\mathcal{B}_d, \mathcal{B}_\#, \psi^2, 0}^{(1)}(\Omega_L), \quad u_{x,2}^{(m)} = u_{\mathcal{B}_n, \mathcal{B}_d, \varphi_x^2, 0}^{(m)}(\Omega_L), \quad \varphi_x = u_{\mathcal{B}_d, \mathcal{B}_\#, 1, V}^{(1)}(\Omega_L),$$

$$(2.18) \quad u_{y,1} = E_x^\# u_{\mathcal{B}_\#, \mathcal{B}_d, \psi^2, 0}^{(1)}(\Omega_1), \quad u_{y,2}^{(m)} = u_{\mathcal{B}_d, \mathcal{B}_n, \varphi_y^2, 0}^{(m)}(\Omega_L), \quad \varphi_y = E_x^\# u_{\mathcal{B}_\#, \mathcal{B}_d, 1, V}^{(1)}(\Omega_1).$$

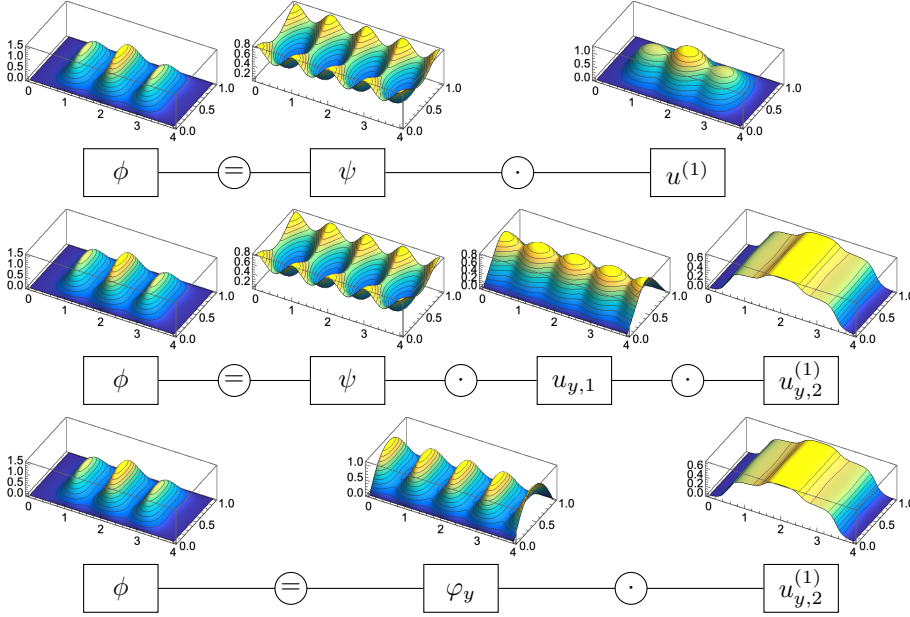


FIG. 2. Visualization of the factorization for the ground state solution of $-\Delta\phi + V\phi = \lambda\phi$, $\phi = 0$ on $\partial\Omega_d$ with $V(x, y) = 10^2(\sin x)^2(\sin y)^2$.

A graphical representation of [Theorem 2.5](#) is presented in [Figure 2](#) for $m = 1$, where the scale separation of, e.g., $\varphi_y^{(1)}$ into a short and $u_{y,2}^{(1)}$ into a large scale is visible. Moreover, the first excited eigenfunctions with $m \in \{2, 3, 4\}$ are visualized in [Figure 3](#). Herein, the m -dependence entirely goes into the $u_{y,2}^{(m)}$ function for the excited eigenfunctions since $\varphi_y^{(1)}$ is fixed.

To prove [Theorem 2.5](#), we need to show that the factorizations are valid changes of variables. The application of the first *factorization principle* in [\(2.12\)](#), i.e.,

$$(2.19) \quad u^{(m)} = u_{\mathcal{B}_d, \mathcal{B}_d, \psi^2, 0}^{(m)} = u_{\mathcal{B}_d, \mathcal{B}_d, 1, V}^{(m)} / \psi,$$

removes the potential V from the eigenvalue problem while still encoding the corresponding information through ψ^2 . The inducing function $\psi = E_x^\# u_{\mathcal{B}_\#, \mathcal{B}_\#, 1, V}^{(1)}(\Omega_1)$ is the solution to a spectral cell problem, and it was shown in [\[5\]](#) that this factorization is indeed a diffeomorphism in $H_0^1(\Omega_L)$. Such factorization operators will apply a change of variables in the min-max characterization of the eigenvalue.

In contrast to [\(2.19\)](#) where ψ^2 is bounded from below a.e. by a positive constant, we will also need factorization operators induced by functions tending to zero at boundary parts due to homogeneous Dirichlet boundary conditions. In such cases, we need to adapt the factorization principle as the boundedness of the division operator is not directly visible, which makes the analysis much more subtle. Thus, we need:

LEMMA 2.6 (Factorization operator with degeneracy and singularity). *Let the inducing function $u_{y,1} := E_x^\# u_{\mathcal{B}_\#, \mathcal{B}_d, \psi^2, 0}^{(1)}(\Omega_1) \in H_{\mathcal{B}_\#, \mathcal{B}_d}^1(\Omega_L)$ with $0 < c < \psi^2 < C$ a.e. be given. Then, the linear factorization operator defined by*

$$(2.20) \quad \begin{aligned} T : H_{\mathcal{B}_d, \mathcal{B}_d}^1(\Omega_L) &\rightarrow H_{\mathcal{B}_d, \mathcal{B}_d}^1(\Omega_L; u_{y,1}^2) \\ u &\mapsto T(u) := z \mapsto u(z)/u_{y,1}(z) \text{ a.e. in } \Omega_L \end{aligned}$$

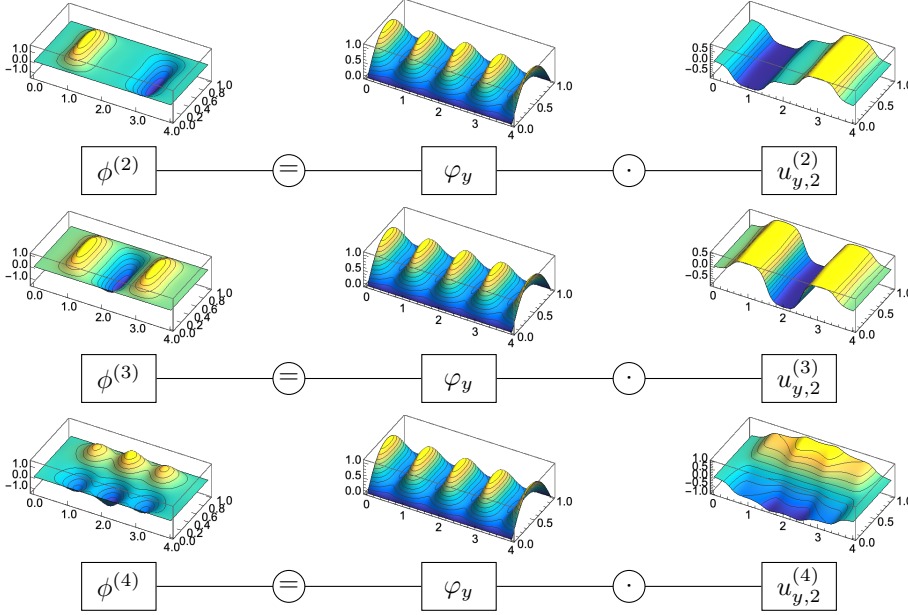


FIG. 3. Visualization of the factorization for some excited states of $-\Delta\phi^{(m)} + V\phi^{(m)} = \lambda^{(m)}\phi^{(m)}$ with $V(x, y) = 10^2(\sin x)^2(\sin y)^2$: By construction, the m -dependence entirely goes into the $u_{y,2}$ contribution.

is bi-continuous and thus a diffeomorphism.

Proof. Noting that T is a division operator, the corresponding multiplication operator T^{-1} is the (left and right) inverse operator. For a simpler notation, we use $H_0^1(\Omega_L) = H_{\mathcal{B}_d, \mathcal{B}_d}^1(\Omega_L)$. So we study

$$(2.21) \quad \begin{aligned} \tilde{T} : H_0^1(\Omega_L) &\rightarrow W & \tilde{T}^{-1} : W &\rightarrow H_0^1(\Omega_L) \\ u &\mapsto u_{y,2} := \tilde{T}(u) = \frac{u}{u_{y,1}} & u_{y,2} &\mapsto u := \tilde{T}^{-1}(u_{y,2}) = u_{y,1}u_{y,2} \end{aligned}$$

with the abstract set $W := \text{Im}(\tilde{T}) = \text{Dom}(\tilde{T}^{-1})$ as

$$(2.22) \quad W = \left\{ u_{y,2} \in \mathcal{D}'(\Omega_L) \mid \exists u \in H_0^1(\Omega_L) : u_{y,2} = \tilde{T}(u) \right\}.$$

We show that the image of \tilde{T} is the $u_{y,1}^2$ -induced space $H_{\mathcal{B}_d, \mathcal{B}_n}^1(\Omega_L; u_{y,1}^2)$. We have $W \subset \mathcal{D}'(\Omega_L)$ since $1/u_{y,1} \in L_{\text{loc}}^1(\Omega_L)$ as $u_{y,1} = 0$ only at the \mathbf{y} -boundary, and therefore $\forall \phi \in \mathcal{D}(\Omega_L) = C_c^\infty(\Omega_L)$, $\tilde{T}(\phi) = \int_{\Omega_L} \frac{1}{u_{y,1}} \phi < \|\phi\|_\infty \int_{\text{supp}(\phi)} \frac{1}{u_{y,1}} < \infty$ is a linear bounded functional since $\text{supp}(\phi)$ is compact. Then we have $W \subset H_{\mathcal{B}_d, \mathcal{B}_n}^1(\Omega_L; u_{y,1}^2)$ since $u_{y,2} \in W$ implies that there exists an $u \in H_0^1(\Omega_L)$, such that $u_{y,2} = \frac{u}{u_{y,1}}$, which yields $\mathcal{B}_d(u_{y,2}) = 0$ on $\partial\Omega_{\mathbf{x}}$ and trivially fulfilled $\mathcal{B}_n(u_{y,2}) = 0$ on $\partial\Omega_{\mathbf{y}}$, and allows us to take

$$(2.23) \quad \tilde{T}^{-1}(u_{y,2}) = \frac{u_{y,1}u_{y,2}}{u_{y,1}} = u_{y,1}u_{y,2} = u \in H_0^1(\Omega_L) \Rightarrow u_{y,2} \in H_{\mathcal{B}_d, \mathcal{B}_n}^1(\Omega_L; u_{y,1}^2).$$

We also have $H_{\mathcal{B}_d, \mathcal{B}_n}^1(\Omega_L; u_{y,1}^2) \subset W$ since $u_{y,2} \in H_{\mathcal{B}_d, \mathcal{B}_n}^1(\Omega_L; u_{y,1}^2)$ implies $\tilde{T}^{-1}(u_{y,2}) =$

$u_{y,1}u_{y,2} = u \in H_0^1(\Omega_L)$ such that

$$(2.24) \quad \exists u \in H_0^1(\Omega_L) : u_{y,2} = \frac{u}{u_{y,1}} = \tilde{T}(u) \Rightarrow u_{y,2} \in W.$$

Thus $W = H_{\mathcal{B}_d, \mathcal{B}_n}^1(\Omega_L; u_{y,1}^2)$, so \tilde{T} defined by from (2.21) coincides with T from (2.20). Moreover, the weighted Sobolev space $H_{\mathcal{B}_d, \mathcal{B}_n}^1(\Omega_L; u_{y,1}^2)$ is a Banach space since $u_{y,1}$ only degenerates on the boundary (c.f. Remark 2.2).

Since T and T^{-1} are both surjective, T is bijective. We now show the continuity of T^{-1} as this is the more straightforward direction being a multiplication operator. Since all $u_{\mathcal{B}_d, \mathcal{B}_d, \psi^2, 0}^{(m)}$ form a basis of $H_0^1(\Omega_L)$ (c.f. subsection 2.1), it suffices to show continuity for all basis functions $u_{\mathcal{B}_d, \mathcal{B}_d, \psi^2, 0}^{(m)}$ and to conclude by the linearity of the operator T^{-1} . Thus, let m be fixed, $u := u_{\mathcal{B}_d, \mathcal{B}_d, \psi^2, 0}^{(m)}$, and $u_{y,2} := T(u_{\mathcal{B}_d, \mathcal{B}_d, \psi^2, 0}^{(m)})$. Then it follows for $u = T^{-1}(u_{y,2}) = u_{y,1}u_{y,2}$ that

$$(2.25) \quad \int_{\Omega_L} \psi^2 \nabla u \cdot \nabla u \, dz = \int_{\Omega_L} \psi^2 (u_{y,1}^2 \nabla u_{y,2} \cdot \nabla u_{y,2} + \nabla u_{y,1} \cdot \nabla (u_{y,2}^2 u_{y,1})) \, dz,$$

which is well defined by the assumption that u is the corresponding eigenfunction for the first expression in (2.25). We further have for the last term in (2.25) that

$$(2.26) \quad \begin{aligned} \int_{\Omega_L} \psi^2 \nabla u_{y,1} \cdot \nabla (u_{y,2}^2 u_{y,1}) \, dz &= - \int_{\Omega_L} \nabla \cdot (\psi^2 \nabla u_{y,1}) u_{y,2}^2 u_{y,1} \, dz \\ &= \lambda_{u_{y,1}}^{(1)} \int_{\Omega_L} (\psi^2 u_{y,1}) (u_{y,2}^2 u_{y,1}) \, dz, \end{aligned}$$

by the definition of $u_{y,1} = E_{\mathbf{x}}^{\#} u_{\mathcal{B}_{\#}, \mathcal{B}_d, \psi^2, 0}^{(1)}(\Omega_1)$ according to (2.8) multiplied with $u_{y,2}^2 u_{y,1}$. Together with $0 < c < \psi^2 < C$, it then follows from (2.25) that

$$(2.27) \quad \begin{aligned} c \int_{\Omega_L} \nabla u \cdot \nabla u \, dz &\leq C \int_{\Omega_L} u_{y,1}^2 \nabla u_{y,2} \cdot \nabla u_{y,2} \, dz + C \lambda_{u_{y,1}}^{(1)} \int_{\Omega_L} u_{y,1}^2 u_{y,2}^2 \, dz \\ &\leq C \max\{1, \lambda_{u_{y,1}}^{(1)}\} \|u_{y,2}\|_{H^1(\Omega_L; u_{y,1}^2)}^2. \end{aligned}$$

Adding $\|u\|_{L^2(\Omega_L)}^2 = \|u_{y,2}\|_{L^2(\Omega_L; u_{y,1}^2)}^2$ on both sides of (2.27) yields

$$(2.28) \quad \|\nabla u\|_{L^2(\Omega_L)}^2 + \|u\|_{L^2(\Omega_L)}^2 \leq \frac{C \max\{1, \lambda_{u_{y,1}}^{(1)}\}}{c} \|u_{y,2}\|_{H^1(\Omega_L; u_{y,1}^2)}^2 + \|u_{y,2}\|_{L^2(\Omega_L; u_{y,1}^2)}^2,$$

which finally, with $u_{y,2} = T(u)$, provides us that $\|u\|_{H^1(\Omega_L)}^2 \leq D \|T(u)\|_{H^1(\Omega_L; u_{y,1}^2)}^2$ for some $D > 0$. This is equivalent to

$$(2.29) \quad \|T^{-1}(u_{y,2})\|_{H^1(\Omega_L)}^2 \leq D \|u_{y,2}\|_{H^1(\Omega_L; u_{y,1}^2)}^2.$$

As T^{-1} is a linear, bijective, and continuous (by (2.29)) operator between two Banach spaces, the inverse $(T^{-1})^{-1} = T$ is also continuous [22, p35] with $\|T(u)\|_{H^1(\Omega_L; u_{y,1}^2)}^2 \leq \tilde{D} \|u\|_{H^1(\Omega_L)}^2$. Bi-continuity of T implies that T and T^{-1} are continuously Fréchet-differentiable since they are both linear. Thus, T is a diffeomorphism [39]. \square

In order to apply the above-defined factorization operator in the min-max setting, we have the following:

LEMMA 2.7 (Rayleigh Quotients after Factorization). *Let $\phi^{(m)} = u_{\mathcal{B}_d, \mathcal{B}_d, 1, V}^{(m)}(\Omega_L)$ and $u^{(m)}, \psi$ be given as in [Theorem 2.5](#). Then, after the factorization of $\phi^{(m)} = u^{(m)} \cdot \psi$, the corresponding Rayleigh quotient reads*

$$(2.30) \quad \mathcal{R}_{1, V}(\phi^{(m)}) = \mathcal{R}_{\psi^2, 0}(u^{(m)}) + \lambda_\psi.$$

Proof. We first note that the factorization allows for the splitting

$$(2.31) \quad \begin{aligned} \nabla \phi^{(m)} \cdot \nabla \phi^{(m)} &= \nabla (u^{(m)} \psi) \cdot \nabla (u^{(m)} \psi) \\ &= \psi^2 \nabla u^{(m)} \cdot \nabla u^{(m)} + \nabla \psi \cdot \nabla \left((u^{(m)})^2 \psi \right). \end{aligned}$$

Using the splitting [\(2.31\)](#), we obtain that $\mathcal{R}_{1, V}(\phi^{(m)})$ is equal to

$$(2.32) \quad \begin{aligned} & \frac{\int_{\Omega_L} \psi^2 \nabla u^{(m)} \cdot \nabla u^{(m)} \, dz}{\int_{\Omega_L} \psi^2 (u^{(m)})^2 \, dz} + \frac{\int_{\Omega_L} \left(\nabla \psi \cdot \nabla \left((u^{(m)})^2 \psi \right) + V \psi \left((u^{(m)})^2 \psi \right) \right) \, dz}{\int_{\Omega_L} \psi \left((u^{(m)})^2 \psi \right) \, dz} \\ &= \mathcal{R}_{\psi^2, 0}(u^{(m)}) + \frac{\int_{\Omega_L} (-\nabla \cdot (\nabla \psi) + V \psi) (u^{(m)})^2 \psi \, dz}{\int_{\Omega_L} \psi \left((u^{(m)})^2 \psi \right) \, dz} \\ &= \mathcal{R}_{\psi^2, 0}(u^{(m)}) + \frac{\int_{\Omega_L} \lambda_\psi \psi \left((u^{(m)})^2 \psi \right) \, dz}{\int_{\Omega_L} \psi \left((u^{(m)})^2 \psi \right) \, dz} = \mathcal{R}_{\psi^2, 0}(u^{(m)}) + \lambda_\psi, \end{aligned}$$

by the definition of the eigenfunction $\psi = E_{\mathbf{x}}^\# u_{\mathcal{B}_\#, \mathcal{B}_d, 1, V}^{(1)}(\Omega_1)$. \square

We can now combine all the above to prove [Theorem 2.5](#):

Proof of [Theorem 2.5](#). For a simpler notation, let $\phi = u_{\mathcal{B}_d, \mathcal{B}_d, 1, V}^{(m)}(\Omega_L)$. We apply the factorization principle twice with

$$(2.33) \quad \phi = u\psi = (T_\psi)^{-1}(u) \quad \text{and} \quad u = u_{y,1} u_{y,2} = (T_{u_{y,1}})^{-1}(u_{y,2}).$$

The operations are defined in [\(2.19\)](#) and [Lemma 2.6](#), and the latter ensures that these are valid changes of variables in the min-max characterization. With [Lemma 2.7](#) and the first change of variables, we then obtain for $\lambda_{\mathcal{B}_d, \mathcal{B}_d, 1, V}^{(m)}(\Omega_L)$ that

$$(2.34) \quad \begin{aligned} \min_{\substack{W_m \subset H_{\mathcal{B}_d, \mathcal{B}_d}^1(\Omega_L) \\ \dim W_m = m}} \max_{\substack{\phi \in W_m \\ \phi \neq 0}} \mathcal{R}_{1, V}(\phi) &= \min_{\substack{W_m \subset H_{\mathcal{B}_d, \mathcal{B}_d}^1(\Omega_L) \\ \dim W_m = m}} \max_{\substack{u \in W_m \\ u \neq 0}} \mathcal{R}_{\psi^2, 0}(u) + \lambda_{\mathcal{B}_\#, \mathcal{B}_\#, 1, V}^{(1)}(\Omega_1) \\ &= \lambda_{\mathcal{B}_d, \mathcal{B}_d, \psi^2, 0}^{(m)}(\Omega_L) + \lambda_{\mathcal{B}_\#, \mathcal{B}_\#, 1, V}^{(1)}(\Omega_1). \end{aligned}$$

The potential V is now encoded in the diffusion coefficient ψ^2 . We now continue in the same fashion with the second factorization and obtain

$$(2.35) \quad \begin{aligned} \lambda_{\mathcal{B}_d, \mathcal{B}_d, \psi^2, 0}^{(m)} &= \min_{\substack{W_m \subset H_{\mathcal{B}_d, \mathcal{B}_d}^1(\Omega_L; u_{y,1}^2) \\ \dim W_m = m}} \max_{\substack{u_{y,2} \in W_m \\ u_{y,2} \neq 0}} \mathcal{R}_{\psi^2 u_{y,1}^2, 0}(u_{y,2}) + \lambda_{\mathcal{B}_\#, \mathcal{B}_d, \psi^2, 0}^{(1)}(\Omega_1) \\ &= \lambda_{\mathcal{B}_d, \mathcal{B}_d, \psi^2 u_{y,1}^2, 0}^{(m)}(\Omega_L) + \lambda_{\mathcal{B}_\#, \mathcal{B}_d, \psi^2, 0}^{(1)}(\Omega_1). \end{aligned}$$

Here, we used $(T_{u_{y,1}})^{-1}(u_{y,2})$ being a diffeomorphism by [Lemma 2.6](#) and, therefore, a well-defined change of variables. The corresponding eigenfunction multiplication in [\(2.13\)](#) is a direct result of the factorizations of [\(2.33\)](#). If we then also apply the ψ -factorization to φ_y , we obtain $\varphi_y = \psi u_{y,1}$ and $\lambda_{\varphi_y} = \lambda_\psi + \lambda_{u_{y,1}}$, which concludes the proof of [\(2.15\)](#). The other relations, i.e. [\(2.12\)](#) and [\(2.14\)](#), follow analogously with applying their respective factorizations $(T(\cdot))^{-1}$ in [\(2.33\)](#). \square

2.3. Homogenization in the Expanding Directions. In order to entirely characterize the asymptotic behavior of the spectrum as $L \rightarrow \infty$, we will now consider the contribution $\lambda_{\mathcal{B}_d, \mathcal{B}_n, \psi^2 u_{y,1,0}^{(m)}(\Omega_L)}$ in [\(2.15\)](#) as the only one that depends on m after the factorization of [Theorem 2.5](#). Then, we can make a precise statement about the asymptotic behavior of this remainder.

THEOREM 2.8 (Asymptotic behavior of expanding direction). *Let $\psi, u_{y,1}$ be given as in [Theorem 2.5](#) and define $\rho := (\psi u_{y,1})^2$. The asymptotic behavior of the eigenpair $u_{\mathcal{B}_d, \mathcal{B}_n, \rho, 0}^{(m)}(\Omega_L), \lambda_{\mathcal{B}_d, \mathcal{B}_n, \rho, 0}^{(m)}(\Omega_L)$ for $L \rightarrow \infty$ is*

$$(2.36) \quad \lambda_{\mathcal{B}_d, \mathcal{B}_n, \rho, 0}^{(m)} = \frac{1}{L^2} \left(\nu^{(m)} + \mathcal{O}\left(\frac{1}{L}\right) \right),$$

$$(2.37) \quad L^{p/2} u_{\mathcal{B}_d, \mathcal{B}_n, \rho, 0}^{(m)}(\mathbf{x}/L, \mathbf{y}) \rightharpoonup u_0^{(m)}(\mathbf{x}) \text{ weakly up to a subseq. in } H_{\mathcal{B}_d, \mathcal{B}_n}^1(\Omega_1),$$

where $(u_0^{(m)}, \nu^{(m)}) \in (H_0^1((0,1)^p) \setminus \{0\}) \times \mathbb{R}$ is the solution to the p -dimensional homogenized eigenvalue problem

$$(2.38) \quad \begin{cases} -\nabla \cdot (\bar{D} \nabla u_0^{(m)}) = \nu^{(m)} \bar{C} u_0^{(m)} & \text{in } (0,1)^p \\ u_0^{(m)} = 0 & \text{on } \partial(0,1)^p \end{cases},$$

with the constant homogenized coefficients, $\bar{D} \in \mathbb{R}^{p \times p}$, $\bar{C} \in \mathbb{R}$, given by

$$(2.39) \quad \bar{D}_{ij} = \int_{(0,1)^p} \int_{(0,\ell)^q} \rho \left(\delta_{ij} + \frac{\partial \theta_j}{\partial x_i} \right) d\mathbf{y} d\mathbf{x}, \quad \bar{C} = \int_{(0,1)^p} \int_{(0,\ell)^q} \rho d\mathbf{y} d\mathbf{x},$$

for $i, j = 1, \dots, p$. The corrector functions $\{\theta_i(\mathbf{x}, \mathbf{y})\}_{1 \leq i \leq p}$ are defined as cell problem solutions on the periodic unit cell, as

$$(2.40) \quad \begin{cases} -\nabla \cdot (\rho(\tilde{\mathbf{x}}, \mathbf{y}) (\mathbf{e}_i + \nabla \theta_i(\tilde{\mathbf{x}}, \mathbf{y}))) = 0 & \text{in } \Omega_1 = (0,1)^p \times (0,\ell)^q \\ \tilde{\mathbf{x}} \mapsto \theta_i(\tilde{\mathbf{x}}, \mathbf{y}) \text{ } \tilde{\mathbf{x}}\text{-periodic} \end{cases}.$$

Furthermore, it holds that $\nu^{(1)} < \nu^{(2)}$.

Proof. The proof is divided into five steps. We first apply a spatial transformation to identify the directional homogenization problem. In the second step, we show the existence of a weakly converging subsequence for the linear source problem. Then, the oscillating test function method provides the homogenized operators whose dimensions can be further reduced by considering the directional framework in the fourth step. The last step transfers the results to the eigenvalue problem.

Step 1: *Identification of a directional homogenization problem by transformation.*

To operate on fixed spatial domains, we map the problem from Ω_L to the reference domain $\Omega_1 = (0,1)^p \times (0,\ell)^q$ by $\mathbf{x} \mapsto \mathbf{x}/L =: \varepsilon \mathbf{x}$ and observe for the transformed weight function $\rho_\varepsilon(\mathbf{x}, \mathbf{y}) := \rho(\mathbf{x}/\varepsilon, \mathbf{y})$ that $1/\rho_\varepsilon \in L_{\text{loc}}^1(\Omega_1)$ and $\rho_\varepsilon > 0$ a.e. in Ω_1 .

Thus, the correct framework is the weighted space $H^1(\Omega_1; \rho_\varepsilon)$. We now encode the Dirichlet boundary conditions on the \mathbf{x} -boundary (as in [50, p6]) in the sense of traces with $\Gamma_D := \{0, 1\}^p \times (0, \ell)^q \subset \partial\Omega_1$ in the subspace

$$(2.41) \quad \mathbb{V}_{\rho_\varepsilon} = \{\phi \in H^1(\Omega_1; \rho_\varepsilon) \mid \phi = 0 \text{ on } \Gamma_D\} \subset H^1(\Omega_1; \rho_\varepsilon).$$

Here, $\mathbb{V}_{\rho_\varepsilon}$ is a Banach space since $\rho_\varepsilon = 0$ occurs only on the boundary Ω_1 (c.f. [Remark 2.2](#)). The weak form of the eigenvalue problem reads: Find $(u_\varepsilon^{(m)}, \lambda_\varepsilon^{(m)}) \in (\mathbb{V}_{\rho_\varepsilon} \setminus \{0\}) \times \mathbb{R}$, such that

$$(2.42) \quad \forall v \in \mathbb{V}_{\rho_\varepsilon} : \quad a_\varepsilon(u_\varepsilon^{(m)}, v) = \lambda_\varepsilon^{(m)} \int_{\Omega_1} \rho_\varepsilon(\mathbf{x}, \mathbf{y}) u_\varepsilon^{(m)} v d\mathbf{x} d\mathbf{y},$$

with the bilinear form

$$(2.43) \quad a_\varepsilon(u_\varepsilon^{(m)}, v) = \int_{\Omega_1} \rho_\varepsilon(\mathbf{x}, \mathbf{y}) \left(\frac{\partial u_\varepsilon^{(m)}}{\partial x_i} \frac{\partial v}{\partial x_i} + \frac{1}{\varepsilon^2} \frac{\partial u_\varepsilon^{(m)}}{\partial y_i} \frac{\partial v}{\partial y_i} \right) d\mathbf{x} d\mathbf{y},$$

using index notation. In (2.42), we moved the ε^2 -scaling to $\lambda_\varepsilon^{(m)}$ as

$$(2.44) \quad \lambda_{\mathcal{B}_d, \mathcal{B}_n, \rho_\varepsilon, 0}^{(m)} = \varepsilon^2 \lambda_\varepsilon^{(m)},$$

which follows from the min-max principle. This operation will be justified later when the existence of this ε^2 -transformed eigenvalue problem is shown for $\varepsilon \rightarrow 0$.

Step 2: *Extraction of a weakly converging subsequence for the linear equation.*

From [46, 47], we know that the homogenization of eigenvalue problems uses the same homogenized operators as for the corresponding source problem. Hence, we consider the bilinear form of the corresponding source problem to derive the homogenized operators. Therefore, given a family $f_\varepsilon(\mathbf{x}, \mathbf{y}) \in \mathbb{V}'_{\rho_\varepsilon}$ with $f_\varepsilon(\mathbf{x}, \mathbf{y}) \rightarrow f_0(\mathbf{x})$ in $\mathbb{V}'_{\rho_\varepsilon}$, we study the variational formulation

$$(2.45) \quad \forall v \in \mathbb{V}_{\rho_\varepsilon} : \quad a_\varepsilon(u_\varepsilon, v) = \langle f_\varepsilon, v \rangle_{\mathbb{V}'_{\rho_\varepsilon} \times \mathbb{V}_{\rho_\varepsilon}}.$$

The restriction of the family f_ε to \mathbf{y} -constant functions in the limit will be justified later when we show that the homogenized limit u_0 will have exactly this form. Thus, since we want to derive the eigenvalue problem from the source problem, f_ε has to mimic the properties of the sequence u_ε . The bilinear form $a_\varepsilon(u_\varepsilon, v)$ is $\mathbb{V}_{\rho_\varepsilon}$ -elliptic (for $\varepsilon \leq 1$), since for all $u_\varepsilon \in \mathbb{V}_{\rho_\varepsilon}$, we have

$$(2.46) \quad \begin{aligned} a_\varepsilon(u_\varepsilon, u_\varepsilon) &\stackrel{\varepsilon \leq 1}{\geq} \|\nabla u_\varepsilon\|_{L^2(\Omega_1; \rho_\varepsilon)}^2 \stackrel{\text{F.-in.}}{\geq} \frac{1}{2} \|\nabla u_\varepsilon\|_{L^2(\Omega_1; \rho_\varepsilon)}^2 + \frac{C_F}{2} \|u_\varepsilon\|_{L^2(\Omega_1; \rho_\varepsilon)}^2 \\ &\geq \frac{1}{2} \min\{1, C_F\} \|u_\varepsilon\|_{H^1(\Omega_1; \rho_\varepsilon)}^2 =: C \|u_\varepsilon\|_{H^1(\Omega_1; \rho_\varepsilon)}^2, \end{aligned}$$

after using the weighted Friedrichs inequality [49, p199] (for homogeneous Dirichlet boundary condition on parts of the boundary). Continuity also holds for all $\varepsilon > 0$ with a continuity constant proportional to $1/\varepsilon^2$. Thus, the problem is well-posed and admits a unique solution for all $\varepsilon > 0$ in $\mathbb{V}_{\rho_\varepsilon}$ (Lax–Milgram, c.f. [27, p126]). We, however, are interested in precisely the limit $\varepsilon \rightarrow 0$, which, at first, seems to be problematic since the continuity constant would tend to infinity if we do not further specify the $\partial\mathbf{y}$ -behavior in (2.43). However, we take (as in [50, p24]) u_ε in the bilinear form and use the coercivity to obtain

$$(2.47) \quad C \|u_\varepsilon\|_{H^1(\Omega_1; \rho_\varepsilon)}^2 \leq a_\varepsilon(u_\varepsilon, u_\varepsilon) = \langle f_\varepsilon, u_\varepsilon \rangle_{\mathbb{V}'_{\rho_\varepsilon} \times \mathbb{V}_{\rho_\varepsilon}} \leq \|f_\varepsilon\|_{H^{-1}(\Omega_1; \rho_\varepsilon)} \|u_\varepsilon\|_{H^1(\Omega_1; \rho_\varepsilon)},$$

with the operator norm $\|f_\varepsilon\|_{H^{-1}(\Omega_1; \rho_\varepsilon)} = \|f_\varepsilon\|_{\mathbb{V}'_{\rho_\varepsilon}} \rightarrow \|f_0\|_{\mathbb{V}'_{\rho_0}} \leq \mathbf{D}$ by our assumption on the family $f_\varepsilon \in \mathbb{V}'_{\rho_\varepsilon}$. Therefore, u_ε is uniformly bounded in $H^1(\Omega_1; \rho_\varepsilon)$ since $\|u_\varepsilon\|_{H^1(\Omega_1; \rho_\varepsilon)} \leq \frac{1}{\mathbf{C}} \|f_\varepsilon\|_{H^{-1}(\Omega_1; \rho_\varepsilon)} < \infty$. Now recall that $\rho_\varepsilon = \rho(\mathbf{x}/\varepsilon, \mathbf{y})$ is \mathbf{x} -periodic and thus weakly converges to its \mathbf{x} -average $\rho_0(\mathbf{y})$ [3, Lem. 1.8.]. From the boundedness of u_ε in $H^1(\Omega_1; \rho_\varepsilon)$, we can follow with [61, Prop. 2.1.] that there exists a $u_0 \in H^1(\Omega_1; \rho_0)$, such that there exists a converging subsequence of u_ε , still denoted by u_ε by abuse of notation, that weakly converges in $H^1(\Omega_1; \rho_0)$. This ensures the existence of the desired homogenized limit u_0 of u_ε as $\varepsilon \rightarrow 0$. We can also directly infer $\sqrt{\rho_\varepsilon} \frac{\partial u_\varepsilon}{\partial \mathbf{y}} \rightarrow \mathbf{0}$ in $L^2(\Omega_1)$ by taking the limit in

$$(2.48) \quad \begin{aligned} \frac{\mathbf{C}}{\varepsilon^2} \int_{\Omega_1} \rho_\varepsilon \left| \frac{\partial u_\varepsilon}{\partial \mathbf{y}} \right|^2 d\mathbf{x} d\mathbf{y} &\leq a_\varepsilon(u_\varepsilon, u_\varepsilon) \\ &\leq \|f_\varepsilon\|_{H^{-1}(\Omega_1; \rho_\varepsilon)} \|u_\varepsilon\|_{H^1(\Omega_1; \rho_\varepsilon)} \leq \frac{1}{\mathbf{C}} \|f_\varepsilon\|_{H^{-1}(\Omega_1; \rho_\varepsilon)}^2 < \infty, \end{aligned}$$

since the norm of u_ε is bounded by the norm of f_ε , which implies that

$$(2.49) \quad \lim_{\varepsilon \rightarrow 0} \left\| \sqrt{\rho_\varepsilon} \frac{\partial u_\varepsilon}{\partial \mathbf{y}} - \mathbf{0} \right\|_{L^2(\Omega_1)} = 0,$$

since $\frac{1}{\mathbf{C}} \|f_\varepsilon\|_{H^{-1}(\Omega_1; \rho_\varepsilon)}^2$ is bounded for all ε , including $\varepsilon = 0$. Therefore, $\sqrt{\rho_\varepsilon} \frac{\partial u_\varepsilon}{\partial \mathbf{y}} \rightarrow \mathbf{0}$ in $L^2(\Omega_1)$, which will be important later to reduce the dimension of the homogenized equation from $p + q$ dimensions to just p . Since ρ_0 is nonzero a.e. on Ω_1 (recall that $\rho_\varepsilon = 0$ only happens on the \mathbf{y} -boundary), we have $\frac{\partial u_\varepsilon}{\partial \mathbf{y}} \rightarrow \mathbf{0}$ in $L^2(\Omega_1)$. Thus, a homogenized limit u_0 with $\partial u_0 / \partial \mathbf{y} = \mathbf{0}$ exists for the sequence u_ε .

Step 3: *Derivation of the homogenized operators using oscillating test functions.*

Since we know that there exists a homogenized limit u_0 , we aim to derive the corresponding homogenized equation for u_0 . Therefore, consider

$$(2.50) \quad \xi_\varepsilon(\mathbf{x}, \mathbf{y}) := \sqrt{\rho_\varepsilon(\mathbf{x}, \mathbf{y})} \nabla u_\varepsilon(\mathbf{x}, \mathbf{y}).$$

Following the usual arguments [50, p24], from the uniform boundedness of u_ε , it follows that

$$(2.51) \quad \|\xi_\varepsilon\|_{L^2(\Omega_1)} = |u_\varepsilon|_{H^1(\Omega_1; \rho_\varepsilon)} \leq \|u_\varepsilon\|_{H^1(\Omega_1; \rho_\varepsilon)} \leq \frac{1}{\mathbf{C}} \|f_\varepsilon\|_{H^{-1}(\Omega_1; \rho_\varepsilon)} < \infty.$$

Therefore, we can again extract subsequences ξ_ε , still denoted by ξ_ε , such that $\xi_\varepsilon \rightharpoonup \xi_0$ in $L^2(\Omega_1)$ weakly. This convergence implies that the equation of interest

$$(2.52) \quad \langle \xi_\varepsilon, \nabla v \rangle_{L^2(\Omega_1)} = \langle f_\varepsilon, v \rangle_{\mathbb{V}_{\rho_\varepsilon}} \quad \forall v \in \mathbb{V}_{\rho_\varepsilon},$$

has a limit for $\varepsilon \rightarrow 0$ as

$$(2.53) \quad \langle \xi_0, \nabla v \rangle_{L^2(\Omega_1)} = \langle f_0, v \rangle_{\mathbb{V}_{\rho_0}} \quad \forall v \in \mathbb{V}_{\rho_0}.$$

To explicitly state this limit equation, we need to calculate ξ_0 . We employ the oscillatory test function method [3, p10] to overcome the problem of $\xi_\varepsilon = \sqrt{\rho(\mathbf{x}/\varepsilon, \mathbf{y})} \nabla u_\varepsilon$ being a product of two weakly converging functions and thus not simply being the product of both limits for $\varepsilon \rightarrow 0$. We need to adapt the method to account for the directional periodicity and the additional ε^{-2} -scaling of the $(\partial u_\varepsilon / \partial y_i)$ -term in the

bilinear form (2.43). Thus, let $\varphi \in \mathcal{D}((0,1)^p)$ be a smooth, only \mathbf{x} -dependent, and compactly supported test function (i.e., $\varphi \in C_c^\infty((0,1)^p)$). Then, inspired by the first two terms in the asymptotic expansion for u_ε , we define the test function φ_ε as

$$(2.54) \quad \varphi_\varepsilon(\mathbf{x}, \mathbf{y}) := \varphi(\mathbf{x}) + \varepsilon \sum_{i=1}^p \frac{\partial \varphi(\mathbf{x})}{\partial x_i} \theta_i(\mathbf{x}/\varepsilon, \mathbf{y})$$

where, with $\tilde{\mathbf{x}} := \mathbf{x}/\varepsilon$, $\theta_i(\tilde{\mathbf{x}}, \mathbf{y})$ is the solution to the corrector problem (2.40), which admits for all $i = 1, \dots, p$ a unique solution $\theta_i \in H^1(\Omega_1; \rho_1) / \mathbb{R}$ (due to periodic boundary conditions). Since $\theta_i(\tilde{\mathbf{x}}, \mathbf{y})$ is $\tilde{\mathbf{x}}$ -periodic, it converges weakly to its average in $H^1(\Omega_1; \rho_0)$ as $\varepsilon \rightarrow 0$. Thus, the expression $\varepsilon \theta_i(\tilde{\mathbf{x}}, \mathbf{y})$ in (2.54) converges to zero since $\varepsilon \rightarrow 0$. This implies that φ_ε has a well-defined limit $\varphi_\varepsilon \rightharpoonup \varphi_0 = \varphi(\mathbf{x})$ for $\varepsilon \rightarrow 0$.

In the following, we group the gradients into (p, q) -blocks by using the notation $\nabla(\cdot) := (\nabla_{\mathbf{x}}(\cdot), \nabla_{\mathbf{y}}(\cdot))^T$. As the derivative of φ_ε is required in the variational formulation, we derive from (2.54), using the chain and product rule, that

$$(2.55) \quad \nabla \varphi_\varepsilon = \sum_{i=1}^p \frac{\partial \varphi(\mathbf{x})}{\partial x_i} \left(e_i + \begin{pmatrix} \nabla_{\tilde{\mathbf{x}}} \theta_i(\tilde{\mathbf{x}}, \mathbf{y}) \\ \varepsilon \nabla_{\mathbf{y}} \theta_i(\tilde{\mathbf{x}}, \mathbf{y}) \end{pmatrix} \right) + \varepsilon \sum_{i=1}^p \begin{pmatrix} \frac{\partial}{\partial x_i} \left(\nabla_{\mathbf{x}} \varphi(\mathbf{x}) \right) \\ 0 \end{pmatrix} \theta_i(\tilde{\mathbf{x}}, \mathbf{y}).$$

We then insert the test function φ_ε into the bilinear form (2.43) to obtain

$$(2.56) \quad \begin{aligned} a_\varepsilon(u_\varepsilon, \varphi_\varepsilon) &= \int_{\Omega_1} \rho_\varepsilon(\mathbf{x}, \mathbf{y}) \nabla u_\varepsilon \cdot \left(\sum_{i=1}^p \frac{\partial \varphi(\mathbf{x})}{\partial x_i} \left(e_i + \begin{pmatrix} \nabla_{\tilde{\mathbf{x}}} \theta_i(\tilde{\mathbf{x}}, \mathbf{y}) \\ \varepsilon^{-1} \nabla_{\mathbf{y}} \theta_i(\tilde{\mathbf{x}}, \mathbf{y}) \end{pmatrix} \right) \right) d\mathbf{x} d\mathbf{y} \\ &+ \varepsilon \int_{\Omega_1} \rho_\varepsilon(\mathbf{x}, \mathbf{y}) \nabla u_\varepsilon \cdot \left(\sum_{i=1}^p \begin{pmatrix} \frac{\partial}{\partial x_i} \left(\nabla_{\mathbf{x}} \varphi(\mathbf{x}) \right) \\ 0 \end{pmatrix} \theta_i(\tilde{\mathbf{x}}, \mathbf{y}) \right) d\mathbf{x} d\mathbf{y}. \end{aligned}$$

The last term in (2.56) vanishes in the limit since it can be bounded by a constant times ε by the Cauchy–Schwarz inequality as the (φ, θ_i) -term is uniformly bounded in $L^2(\Omega_1; \rho_\varepsilon)$ by uniform boundedness of the data in (2.40) and φ -smoothness. The other term, ∇u_ε , is uniformly bounded in $L^2(\Omega_1; \rho_\varepsilon)$ by (2.51). Integration by parts (with Dirichlet in \mathbf{x} - and trivially fulfilled Neumann data in \mathbf{y} -direction) in the other term of (2.56) yields

$$(2.57) \quad \begin{aligned} &\int_{\Omega_1} \rho_\varepsilon(\mathbf{x}, \mathbf{y}) \nabla u_\varepsilon \cdot \left(\sum_{i=1}^p \frac{\partial \varphi(\mathbf{x})}{\partial x_i} \left(e_i + \begin{pmatrix} \nabla_{\tilde{\mathbf{x}}} \theta_i(\tilde{\mathbf{x}}, \mathbf{y}) \\ \varepsilon^{-1} \nabla_{\mathbf{y}} \theta_i(\tilde{\mathbf{x}}, \mathbf{y}) \end{pmatrix} \right) \right) d\mathbf{x} d\mathbf{y} \\ &= - \int_{\Omega_1} u_\varepsilon \nabla \cdot \left(\rho_\varepsilon(\mathbf{x}, \mathbf{y}) \sum_{i=1}^p \frac{\partial \varphi(\mathbf{x})}{\partial x_i} \left(e_i + \begin{pmatrix} \nabla_{\tilde{\mathbf{x}}} \theta_i(\tilde{\mathbf{x}}, \mathbf{y}) \\ \varepsilon^{-1} \nabla_{\mathbf{y}} \theta_i(\tilde{\mathbf{x}}, \mathbf{y}) \end{pmatrix} \right) \right) d\mathbf{x} d\mathbf{y}. \end{aligned}$$

The divergence term in (2.57) can be further simplified to

$$(2.58) \quad \begin{aligned} &\nabla \cdot \left(\rho_\varepsilon(\mathbf{x}, \mathbf{y}) \sum_{i=1}^p \frac{\partial \varphi(\mathbf{x})}{\partial x_i} \left(e_i + \begin{pmatrix} \nabla_{\tilde{\mathbf{x}}} \theta_i(\tilde{\mathbf{x}}, \mathbf{y}) \\ \varepsilon^{-1} \nabla_{\mathbf{y}} \theta_i(\tilde{\mathbf{x}}, \mathbf{y}) \end{pmatrix} \right) \right) \\ &= \sum_{i=1}^p \frac{\partial}{\partial x_i} \begin{pmatrix} \nabla_{\mathbf{x}} \varphi(\mathbf{x}) \\ 0 \end{pmatrix} \cdot \rho_\varepsilon(\mathbf{x}, \mathbf{y}) \left(e_i + \begin{pmatrix} \nabla_{\tilde{\mathbf{x}}} \theta_i(\tilde{\mathbf{x}}, \mathbf{y}) \\ 0 \end{pmatrix} \right) \\ &+ \varepsilon^{-1} \sum_{i=1}^p \frac{\partial \varphi(\mathbf{x})}{\partial x_i} \left[\begin{pmatrix} \nabla_{\tilde{\mathbf{x}}} \\ \nabla_{\mathbf{y}} \end{pmatrix} \cdot \left(\rho(\tilde{\mathbf{x}}, \mathbf{y}) \left(e_i + \begin{pmatrix} \nabla_{\tilde{\mathbf{x}}} \\ \nabla_{\mathbf{y}} \end{pmatrix} \theta_i(\tilde{\mathbf{x}}, \mathbf{y}) \right) \right) \right], \end{aligned}$$

From (2.58), we extract

$$(2.59) \quad \varepsilon^{-1} \left(\frac{\nabla_{\tilde{\mathbf{x}}}}{\nabla_{\mathbf{y}}} \right) \cdot \left(\rho(\tilde{\mathbf{x}}, \mathbf{y}) \left(e_i + \left(\frac{\nabla_{\tilde{\mathbf{x}}}}{\nabla_{\mathbf{y}}} \right) \theta_i(\tilde{\mathbf{x}}, \mathbf{y}) \right) \right),$$

which is zero (even for $\varepsilon \rightarrow 0$) due to the particular definition of the correctors θ_i in (2.40). Here, we notice that the ε^{-2} -scaling in the \mathbf{y} -term of the initial expression precisely aligns with the extruding additional ε^{-1} that appeared in (2.59) by the chain rule. Thus, the only remaining term of (2.58) is

$$(2.60) \quad \sum_{i=1}^p \frac{\partial}{\partial x_i} \left(\frac{\nabla_{\mathbf{x}} \varphi(\mathbf{x})}{0} \right) \cdot \rho_{\varepsilon}(\mathbf{x}, \mathbf{y}) \left(e_i + \left(\frac{\nabla_{\tilde{\mathbf{x}}} \theta_i(\tilde{\mathbf{x}}, \mathbf{y})}{0} \right) \right),$$

which is bounded in $L^2(\Omega_1)$ and, thus, weakly converges as $\varepsilon \rightarrow 0$ to its average in the $\tilde{\mathbf{x}}$ -direction [3, Lem. 1.8.].

In (2.57), now recall that u_{ε} converges strongly to u_0 in $L^2(\Omega_1; \rho_0)$ (by the Rellich theorem, c.f. [2, Thm. 4.3.21]). Thus, we can take the limit of the right-hand side in (2.57). So in total, we can take the limit of (2.56), which is the product of the limit of $u_{\varepsilon} \rightarrow u_0$ (strongly) with the weak limit (2.60) of the divergence term. Thus the weak form (2.45) reduces for $\varepsilon \rightarrow 0$ to

$$(2.61) \quad \begin{aligned} & - \int_{\Omega_1} u_0(\mathbf{x}) \nabla \cdot \left(\int_{(0,1)^p} \rho(\tilde{\mathbf{x}}, \mathbf{y}) \sum_{i=1}^p \frac{\partial \varphi(\mathbf{x})}{\partial x_i} \left(e_i + \left(\frac{\nabla_{\tilde{\mathbf{x}}} \theta_i(\tilde{\mathbf{x}}, \mathbf{y})}{0} \right) \right) d\tilde{\mathbf{x}} \right) d\mathbf{x} d\mathbf{y} \\ &= \lim_{\varepsilon \rightarrow 0} \int_{\Omega_1} \rho_{\varepsilon}(\mathbf{x}, \mathbf{y}) \nabla u_{\varepsilon}(\mathbf{x}, \mathbf{y}) \cdot \nabla \varphi_{\varepsilon}(\mathbf{x}, \mathbf{y}) d\mathbf{x} d\mathbf{y} \\ &= \lim_{\varepsilon \rightarrow 0} \int_{\Omega_1} \rho_{\varepsilon}(\mathbf{x}, \mathbf{y}) f_{\varepsilon}(\mathbf{x}, \mathbf{y}) \varphi_{\varepsilon}(\mathbf{x}, \mathbf{y}) d\mathbf{x} d\mathbf{y} \\ &= \int_{\Omega_1} \rho_0(\mathbf{y}) f_0(\mathbf{x}) \varphi(\mathbf{x}) d\mathbf{x} d\mathbf{y}. \end{aligned}$$

We can rewrite the left-hand side of (2.61) using a compact notation as

$$(2.62) \quad \begin{aligned} & \left[\int_{(0,1)^p} \rho(\tilde{\mathbf{x}}, \mathbf{y}) \sum_{i=1}^p \frac{\partial \varphi(\mathbf{x})}{\partial x_i} \left(e_i + \left(\frac{\nabla_{\tilde{\mathbf{x}}} \theta_i(\tilde{\mathbf{x}}, \mathbf{y})}{0} \right) \right) d\tilde{\mathbf{x}} \right]_j \\ &= \sum_{i=1}^p \frac{\partial \varphi(\mathbf{x})}{\partial x_i} \int_{(0,1)^p} \rho(\tilde{\mathbf{x}}, \mathbf{y}) \left(\delta_{ij} + \frac{\partial \theta_i}{\partial \tilde{x}_j} \right) d\tilde{\mathbf{x}} =: \sum_{i=1}^p \frac{\partial \varphi(\mathbf{x})}{\partial x_i} \tilde{D}_{ji}(\mathbf{y}), \end{aligned}$$

where we identify the last expression as $[\tilde{D}^T(\mathbf{y}) \nabla \varphi(\mathbf{x})]_j$. As the last step, we reverse the integration by parts and obtain the variational formulation of the homogenized equation for u_0 , which is still posed on the $(p+q)$ -dimensional domain Ω_1 , but with u_0 only \mathbf{x} -dependent according to (2.49). The problem then reads: Find $u_0(\mathbf{x}) \in \mathbb{V}_{\rho_0}$, such that

$$(2.63) \quad \int_{\Omega_1} \tilde{D}(\mathbf{y}) \nabla u_0(\mathbf{x}) \cdot \nabla \varphi(\mathbf{x}) d\mathbf{x} d\mathbf{y} = \int_{\Omega_1} \tilde{C}(\mathbf{y}) f_0(\mathbf{x}) \varphi(\mathbf{x}) d\mathbf{x} d\mathbf{y} \quad \forall \varphi \in C_c^{\infty}((0,1)^p),$$

with the \mathbf{y} -dependent operators

$$(2.64) \quad \tilde{D}_{ij}(\mathbf{y}) = \int_{(0,1)^p} \rho(\tilde{\mathbf{x}}, \mathbf{y}) \left(\delta_{ij} + \frac{\partial \theta_j}{\partial \tilde{x}_i} \right) d\tilde{\mathbf{x}}, \quad \tilde{C}(\mathbf{y}) = \int_{(0,1)^p} \rho(\tilde{\mathbf{x}}, \mathbf{y}) d\tilde{\mathbf{x}},$$

for $i, j = 1, \dots, p$. In (2.64), we remark that these operators look very similar to the usual homogenized operators, e.g., in [5], with the difference that the integration only takes place in the p expanding directions over $(0, 1)^p$.

Step 4: *Dimension reduction of the homogenized linear equation.*

In our setup, we can, however, further reduce the homogenized limit equation (2.63) since, by definition, $\nabla\varphi(\mathbf{x}) = (\nabla_{\mathbf{x}}\varphi(\mathbf{x}), 0)^T$. This allows us to concretize further that $u_0(\mathbf{x}) \in H_0^1((0, 1)^p)$ since $u_0(\mathbf{x}) \in \mathbb{V}_{\rho_0(\mathbf{y})}$ implies $u_0(\mathbf{x}) = 0$ on $\partial(0, 1)^p$ and $\|u_0(\mathbf{x})\|_{H^1((0, 1)^p)} < \infty$ since for any $u(\mathbf{x}) \in H^1(\Omega_1; \rho_0)$ with $\rho_0(\mathbf{y}) > 0$ a.e. in $(0, \ell)^q$, it holds that

$$(2.65) \quad \|u(\mathbf{x})\|_{H^1(\Omega_1; \rho_0)}^2 = \left(\int_{(0, 1)^q} \rho_0(\mathbf{y}) d\mathbf{y} \right) \|u(\mathbf{x})\|_{H^1((0, 1)^p)}^2 = \overline{\rho_0^y} \|u(\mathbf{x})\|_{H^1((0, 1)^p)}^2 < \infty,$$

since $\overline{\rho_0^y} \in \mathbb{R}$ is a strictly positive constant. Thus, the homogenized equation reduces from the $(p + q)$ - to the p -dimensional variational problem: Find $u_0 \in H_0^1((0, 1)^p)$, such that

$$(2.66) \quad \int_{(0, 1)^p} \bar{D} \nabla u_0(\mathbf{x}) \cdot \nabla \varphi(\mathbf{x}) d\mathbf{x} = \int_{(0, 1)^p} \bar{C} f_0(\mathbf{x}) \varphi(\mathbf{x}) d\mathbf{x} \quad \forall \varphi \in C_c^\infty((0, 1)^p),$$

with the constant homogenized coefficients, defined by (2.39) as the integral of $\tilde{C}(\mathbf{y})$ and $\tilde{D}(\mathbf{y})$ from (2.64) over $(0, 1)^q$.

The homogenized equation (2.66) is formulated on $H_0^1((0, 1)^p)$. Recall that the test function $\varphi \in C_c^\infty((0, 1)^p)$ was chosen arbitrarily. Since $C_c^\infty((0, 1)^p)$ is dense in $H_0^1((0, 1)^p)$ by the definition of H_0^1 as the closure of C_c^∞ under the H^1 -norm [2, Def. 4.3.8.], (2.63) holds $\forall \varphi \in H_0^1((0, 1)^p)$. As the homogenized operator satisfies coercivity (c.f. [50, Rem. 2.6.]), the theorem of Lax–Milgram ensures the uniqueness of the homogenized limit u_0 . This, on the other hand, implies that any subsequence of u_ε converges to u_0 in the limit. Thus, the entire sequence u_ε converges to the same limit u_0 following the standard arguments from, e.g., [3].

Step 5: *Derivation of the homogenized eigenvalue equation.*

Since we now have derived the homogenized equation for the source problem, we can directly deduce from [46, Thm. 2.1.] that the eigenvalues and -functions converge to the homogenized eigenvalue equation, posed with the same operator as in (2.66), resulting in

$$(2.67) \quad (\lambda_\varepsilon^{(m)}, u_\varepsilon^{(m)}) \rightarrow (\nu^{(m)}, u_0^{(m)}) \text{ in } \mathbb{R} \times (H_0^1((0, 1)^p) \text{ weakly up to subseq.}),$$

where the homogenized eigenpair is defined through (2.38). We furthermore have $\lambda_\varepsilon^{(m)} = \nu^{(m)} + \mathcal{O}(\varepsilon)$ [47, p201] [52, p1638] [8, p942]. The convergence of the eigenfunctions holds up to a subsequence because of the eigenvalue multiplicity of the homogenized limit. To account for the normalization constraint after the initial transformation of $\mathbf{x} \mapsto \varepsilon \mathbf{x}$, we note that $\|u_0(\cdot, \cdot)\|_{L^2(\Omega_L)} = L^{p/2} \|u_0(\cdot/L, \cdot)\|_{L^2(\Omega_1)}$ by the transformation rule and recall the $(1/L^2)$ -scaling from (2.44) for the eigenvalues, which implies (2.36).

The limit eigenvalue $\nu^{(m)}$ is simple and $\nu^{(1)} < \nu^{(2)} < \nu^{(3)} < \dots \rightarrow \infty$ by the Sturm–Liouville theory for the particular case of $p = 1$ with $\bar{D}_{11}, \bar{C} > 0$. Furthermore, we have $\nu^{(1)} < \nu^{(2)} \leq \nu^{(3)} \leq \dots \rightarrow \infty$ for the general case of $p \geq 2$ since the eigenvalue problem is elliptic. However, multiplicities could exceed one for higher eigenvalues. \square

We are now ready to prove the quasi-optimality of the spectral shift $\sigma = \lambda_{\varphi_y}$:

THEOREM 2.9. *For the quasi-optimal shift $\sigma = \lambda_{\varphi_y} = \lambda_{\mathcal{B}_{\#}, \mathcal{B}_{d,1}, V}^{(1)}(\Omega_1)$, the asymptotic shifted fundamental eigenvalue ratio of the linear periodic Schrödinger eigenvalue problem (1.2) converges to a positive constant $C < 1$ as $L \rightarrow \infty$, that is*

$$(2.68) \quad 0 \leq \frac{\lambda_{\mathcal{B}_d, \mathcal{B}_{d,1}, V}^{(1)}(\Omega_L) - \lambda_{\mathcal{B}_{\#}, \mathcal{B}_{d,1}, V}^{(1)}(\Omega_1)}{\lambda_{\mathcal{B}_d, \mathcal{B}_{d,1}, V}^{(2)}(\Omega_L) - \lambda_{\mathcal{B}_{\#}, \mathcal{B}_{d,1}, V}^{(1)}(\Omega_1)} = \frac{\lambda_{\mathcal{B}_d, \mathcal{B}_n, \varphi_y^2, 0}^{(1)}(\Omega_L)}{\lambda_{\mathcal{B}_d, \mathcal{B}_n, \varphi_y^2, 0}^{(2)}(\Omega_L)} \rightarrow C < 1.$$

Proof. The proof follows from [Theorem 2.8](#) since $L^2 \lambda_{\mathcal{B}_d, \mathcal{B}_n, \varphi_y^2, 0}^{(m)}(\Omega_L) = \nu^{(m)} + o(\frac{1}{L})$ and $\nu^{(1)} < \nu^{(2)}$. \square

We will see later that pre-asymptotic effects lead to a non-monotonic convergence of (2.68). However, since the convergence holds in the limit, we can make a statement for uniform boundedness if L is sufficiently large.

COROLLARY 2.10. *There exists a constant $D \in [0, 1)$ and a length $L^* \in \mathbb{R}^+$, such that the quasi-optimally shifted ratio from [Theorem 2.9](#) is uniformly bounded from above by D for all $L > L^*$. That is*

$$(2.69) \quad 0 \leq \frac{\lambda_{\mathcal{B}_d, \mathcal{B}_{d,1}, V}^{(1)}(\Omega_L) - \lambda_{\mathcal{B}_{\#}, \mathcal{B}_{d,1}, V}^{(1)}(\Omega_1)}{\lambda_{\mathcal{B}_d, \mathcal{B}_{d,1}, V}^{(2)}(\Omega_L) - \lambda_{\mathcal{B}_{\#}, \mathcal{B}_{d,1}, V}^{(1)}(\Omega_1)} < D < 1 \quad \forall L > L^*.$$

Proof. The proof follows directly from the convergence result of [Theorem 2.9](#). \square

Remark 2.11. The quasi-optimal shift $\sigma = \lambda_{\mathcal{B}_d, \mathcal{B}_{d,1}, V}^{(1)}(\Omega_L)$ does not affect the absolute eigenvalue ordering in the sense that $0 < |\lambda_L^{(1)} - \sigma| < |\lambda_L^{(2)} - \sigma| \leq |\lambda_L^{(3)} - \sigma| \leq \dots \rightarrow \infty$ since all $\lambda_L^{(i)}$ are positive and $\sigma < \lambda_L^{(1)}$. This property ensures, for example, that the unshifted and the σ -shifted inverse power method (see [Definition 3.1](#)) always converge to the same eigenpair.

[Theorem 2.8](#) gives an abstract description of the homogenized equation. However, for our present setup, we can even solve the equation analytically (which will be important later in [subsection 4.1](#)):

Remark 2.12. The homogenization problem in [Theorem 2.8](#) is posed with an isotropic operator ρI , and ρ is either periodic or zero on the unit cell boundaries $\partial\Omega_1$. Thus, every column of ρI is a solenoidal vector field in Ω_1 in the integral sense by the divergence theorem. Hence, we can conclude with [\[45, p17\]](#) that the homogenized operator is diagonal. Then, the diagonality allows us to explicitly state the homogenized eigenpairs as the Laplacian eigenfunctions on the hyper rectangle with scaled Laplacian eigenvalues as $\nu^{(m)} = \pi^2 (\sum_{i=1}^p \bar{D}_{ii} m_i^2) / \bar{C}$ and $u^{(m)}(\mathbf{x}) = \mathcal{N}^{(m)} \prod_i^p \sin(m_i \pi x_i)$, where the set $\mathcal{M} = \{m_1, \dots, m_p\} \in \mathbb{N}^p$, $|\mathcal{M}| = m$, is chosen to minimize $\nu^{(m)}$. The $\mathcal{N}^{(m)}$ factors are defined by the normalization condition $\int_{(0,1)^p} \bar{C} (u^{(m)})^2 = 1$.

We now return to the convergence properties of the eigenvalue solvers. [Theorem 2.9](#) implies a constant number of iterations for all eigensolvers that are shift-and-invert preconditioned with $\sigma = \lambda_{\mathcal{B}_{\#}, \mathcal{B}_{d,1}, V}^{(1)}(\Omega_1)$ and depend on the fundamental ratio. With this strategy, the eigensolver can reach a given residual norm with a constant number of iterations for all $L \rightarrow \infty$.

3. Spatial Discretization and Iterative Eigensolvers. To solve the eigenvalue problem (1.2) numerically, we will discretize the continuous equation on a finite-dimensional space. Then, we solve the resulting system with a preconditioned algebraic eigensolver.

3.1. Galerkin Finite Element Approach. Consider a conforming and shape-regular partition \mathcal{T}_h of the domain Ω_L into finite elements $\tau \in \mathcal{T}_h$, which have a polygonal shape. We write \mathcal{T}_h for partitions where every element has a diameter of at most $2h$ [53, p36]. Define the finite element subspace $\mathbb{H}_h(\Omega_L) \subset H_0^1(\Omega_L)$, consisting of polynomial functions with total degree r from the polynomial space \mathcal{P}_r , to be $\mathbb{H}_h(\Omega_L) = \{u \in H_0^1(\Omega_L) \mid u|_\tau \in \mathcal{P}_r(\tau) \forall \tau \in \mathcal{T}_h\}$. We then search for a discrete solution $\phi_h^{(m)} \in (\mathbb{H}_h(\Omega_L) \setminus \{0\})$, such that

$$(3.1) \quad \forall v_h \in \mathbb{H}_h(\Omega_L) : \quad \int_{\Omega_L} \nabla \phi_h^{(m)} \cdot \nabla v_h \, dz + \int_{\Omega_L} V \phi_h^{(m)} v_h \, dz = \lambda_h^{(m)} \int_{\Omega_L} \phi_h^{(m)} v_h \, dz.$$

Let now $\mathbf{x}_h^{(m)}$ be the coefficient vector that represents $\phi_h^{(m)}$ in a given basis of $\mathbb{H}_h(\Omega_L)$. We then obtain the equivalent generalized algebraic eigenvalue problem: Find $\mathbf{x}_h^{(m)} \in \mathbb{R}^n \setminus \{\mathbf{0}\}$, such that

$$(3.2) \quad \mathbf{A} \mathbf{x}_h^{(m)} = \lambda_h^{(m)} \mathbf{B} \mathbf{x}_h^{(m)},$$

where $\mathbf{A} \in \mathbb{R}^{n \times n}$ consists of the usual stiffness matrix plus the contribution from the potential, and $\mathbf{B} \in \mathbb{R}^{n \times n}$ denotes the mass matrix. Both \mathbf{A} and \mathbf{B} as finite representations of the continuous operators in (1.2) are symmetric positive definite. Since the discrete problem is formulated on a subspace $\mathbb{H}_h(\Omega_L) \subset H_0^1(\Omega_L)$, we have by the min-max characterization that $\lambda^{(m)} \leq \lambda_h^{(m)}$. Furthermore, we have $\lambda_h^{(m)} \rightarrow \lambda^{(m)}$ for $h \rightarrow 0$ [18, 53].

For the calculation of the quasi-optimal shift λ_{φ_y} , we solve

$$(3.3) \quad \forall v_h \in \mathbb{H}_h^{\varphi_y}(\Omega_1) : \quad \int_{\Omega_1} \nabla \varphi_{y,h}^{(1)} \cdot \nabla v_h \, dz + \int_{\Omega_1} V \varphi_{y,h}^{(1)} v_h \, dz = \lambda_{\varphi_y,h}^{(1)} \int_{\Omega_L} \varphi_{y,h}^{(1)} v_h \, dz,$$

where $\mathbb{H}_h^{\varphi_y}(\Omega_1) := \{u \in H_{\mathcal{B}_{\#}, \mathcal{B}_d}^1(\Omega_1) \mid u|_\tau \in \mathcal{P}_r(\tau) \forall \tau \in (\mathcal{T}_h \cap \Omega_1)\}$ with the same \mathcal{T}_h and r as for $\mathbb{H}_h(\Omega_L)$ (assuming Ω_1 -aligned elements).

3.2. Quasi-Optimally Preconditioned Eigenvalue Algorithms. To solve the resulting discrete eigenvalue problem (3.2), we use the analytic results from section 2 to obtain the quasi-optimal shift as

$$(3.4) \quad \sigma = \lambda_\infty = \lim_{L \rightarrow \infty} \lambda_L^{(1)} = \lambda_{\varphi_y} \approx \lambda_{\varphi_y,h}^{(1)},$$

by combining the results of Theorems 2.5 and 2.8. Using σ , we construct the preconditioner $\mathbf{P} = (\mathbf{A} - \sigma \mathbf{B})^{-1}$. With the generalized Rayleigh quotient $R_{\mathbf{A}, \mathbf{B}}(\mathbf{x}) = (\mathbf{x}^T \mathbf{A} \mathbf{x}) / (\mathbf{x}^T \mathbf{B} \mathbf{x})$, we define:

DEFINITION 3.1 (Shifted Inverse Power Method, IP_σ). *Let $\mathbf{A}, \mathbf{B} \in \mathbb{R}^{n \times n}$ and a start vector $\mathbf{x}_0 \in \mathbb{R}^n$ be given, repeat*

$$(3.5) \quad \tilde{\mathbf{x}}_k = \mathbf{P} \mathbf{B} \mathbf{x}_{k-1}, \quad \mathbf{x}_k = \tilde{\mathbf{x}}_k / \sqrt{\tilde{\mathbf{x}}_k^T \mathbf{B} \tilde{\mathbf{x}}_k}, \quad \lambda_k = R_{\mathbf{A}, \mathbf{B}}(\mathbf{x}_k),$$

until $\|\mathbf{A} \mathbf{x}_k - \lambda_k \mathbf{B} \mathbf{x}_k\|_2 < \text{TOL}$ or $k > k_{max}$.

DEFINITION 3.2 (Locally Optimal Preconditioned Conjugate Gradient Method, LOPCG_σ). *Let $\mathbf{A}, \mathbf{B} \in \mathbb{R}^{n \times n}$ and the start vectors $\mathbf{x}_{-1}, \mathbf{x}_0 \in \mathbb{R}^n$ be given, repeat*

$$(3.6) \quad \mathbf{w}_k = \mathbf{P}(\mathbf{A} \mathbf{x}_{k-1} - R_{\mathbf{A}, \mathbf{B}}(\mathbf{x}_{k-1}) \mathbf{B} \mathbf{x}_{k-1}), \quad S_k = \text{span}(\{\mathbf{x}_{k-1}, \mathbf{w}_k, \mathbf{x}_{k-2}\})$$

$$\tilde{\mathbf{x}}_k = \arg \min_{\mathbf{y} \in S_k} R_{\mathbf{A}, \mathbf{B}}(\mathbf{y}), \quad \mathbf{x}_k = \tilde{\mathbf{x}}_k / \sqrt{\tilde{\mathbf{x}}_k^T \mathbf{B} \tilde{\mathbf{x}}_k}, \quad \lambda_k = R_{\mathbf{A}, \mathbf{B}}(\mathbf{x}_k),$$

until $\|\mathbf{A} \mathbf{x}_k - \lambda_k \mathbf{B} \mathbf{x}_k\|_2 < \text{TOL}$ or $k > k_{max}$.

In (3.6), the locally optimal step is calculated by minimizing in a 3-dimensional subspace with the standard Rayleigh–Ritz method [20] as $\tilde{\mathbf{x}}_k = \alpha_1 \mathbf{x}_{k-1} + \alpha_2 \mathbf{w}_k + \alpha_3 \mathbf{x}_{k-2}$, where the coefficients $\boldsymbol{\alpha} \in \mathbb{R}^3$ are derived from the smallest eigenpair solution of the 3-dimensional eigenvalue problem $\mathbf{V}^T \mathbf{A} \mathbf{V} \boldsymbol{\alpha} = \lambda^{(1)} \mathbf{V}^T \mathbf{B} \mathbf{V} \boldsymbol{\alpha}$ with $\mathbf{V} = [\mathbf{x}_{k-1} \ \mathbf{w}_k \ \mathbf{x}_{k-2}] \in \mathbb{R}^{n \times 3}$.

The above two methods represent the class of gap-dependent iterative eigenvalue algorithms. Optimization-inspired Riemannian gradient algorithms also depend on the fundamental ratio [42, Thm. 3.2]. Alternative approaches, such as the Rayleigh quotient iteration or block algorithms, are not considered in our setup since the former has no guaranteed convergence to the ground state [20, p53]. At the same time, the latter requires an L -proportional block size to retain a quasi-optimal convergence [20, p54].

4. Numerical Experiments. This section concerns the numerical evaluation of the proposed eigensolver preconditioner. We implemented our method using the `Gridap` [19] framework in the Julia programming language [21]. `Gridap` turned out to be a very well-suited framework for our tests since it allowed us to quickly implement weak formulations in a high-level fashion, similar to the `FEniCS` [10, 56] framework in Python. For reproducibility, we provide all examples publicly in [55].

4.1. Homogenization of a Degenerate Eigenvalue Problem with Two Expanding Directions in Three Dimensions. Before we employ the constructed preconditioner for the linear Schrödinger eigenvalue problem (1.2), we first investigate the homogenization results of Theorem 2.8 since these results can be applied and studied independently. Thus, the theoretical predictions about the convergence of the m -dependent contribution $u_{\mathcal{B}_d, \mathcal{B}_n, \rho, 0}^{(m)}(\Omega_L), \lambda_{\mathcal{B}_d, \mathcal{B}_n, \rho, 0}^{(m)}(\Omega_L)$ in three dimensions ($p = 2, q = 1$) are studied numerically. We prescribe the weight function by

$$(4.1) \quad \rho(\mathbf{x}, \mathbf{y}) = \left(\frac{27}{4} y_1^2 (1 - y_1) \left(10 \cos(\pi x_1)^2 + 10 \cos(\pi x_2)^2 + \frac{11}{10} - \sin(\pi y_1)^2 \right) \right)^2.$$

Note that we do not set $\rho = (\psi u_{y,1})$ as in Theorem 2.8 since we want to demonstrate the results for the more general case of ρ not being induced by eigenfunctions but only satisfying the periodicity- and zero-condition on the \mathbf{x} - and \mathbf{y} -boundary respectively. The weight function ρ in (4.1) is positive a.e. and vanishes only on the \mathbf{y} -boundary. By construction, ρ is \mathbf{x} -periodic, thus fulfilling all requirements of Theorem 2.8. We intentionally use the \mathbf{x} -symmetry also to confirm the convergence of degenerate eigenpairs. For a better evaluation, we do not solve for Ω_L but solve an equivalent problem on the reference domain Ω_1 , where we factorized the $(1/L^2)$ -scaling (see Theorem 2.8) of the eigenvalue without affecting the eigenfunctions. To be precise, we check if the solution to

$$(4.2) \quad \begin{cases} -\nabla \cdot \left(\rho(L\mathbf{x}, \mathbf{y}) \operatorname{diag}(1, 1, \frac{1}{L^2}) \nabla u_{1/L}^{(m)} \right) = \lambda_{1/L}^{(m)} \rho(L\mathbf{x}, \mathbf{y}) u_{1/L}^{(m)} & \text{in } (0, 1)^3 \\ u_{1/L}^{(m)} = 0 & \text{on } \partial(0, 1)^2 \times (0, 1) \end{cases},$$

converge to $(u_0^{(m)}, \nu^{(m)})$ from (2.38) in the limit for $L \rightarrow \infty$. The calculation of this homogenized limit first needs the corrector functions to define the homogenized operators. Thus, we solve the corrector equation (2.40) using \mathbb{Q}_2 finite elements on a structured mesh with 300 intervals per direction. These corrector solutions allow the construction of the homogenized coefficients (according to (2.38) and (2.39)) with $\bar{D} \approx \operatorname{diag}(38.75893, 38.75893)$ and $\bar{C} \approx 57.86864$. We observe that $\bar{D}_{11} = \bar{D}_{22}$ as

the result of choosing an (x_1, x_2) -symmetric weight function ρ . The homogenized diffusion matrix is diagonal since we have $\int_{\Omega_1} \nabla \cdot (\rho I) = 0$ by the divergence theorem as ρ defined by (4.1) is either periodic or zero on the boundary of the unit cube, which resembles the case of Remark 2.12. Therefore, we can solve the homogenized equation analytically (with the expressions from Remark 2.12) to obtain

$$(4.3) \quad \begin{aligned} \nu^{(1)} &= \frac{\pi^2 (1^2 \bar{D}_{11} + 1^2 \bar{D}_{22})}{\bar{C}} = \frac{2\pi^2 \bar{D}_{11}}{\bar{C}}, \quad \nu^{(2)} = \nu^{(3)} = \frac{5\pi^2 \bar{D}_{11}}{\bar{C}}, \quad \nu^{(4)} = \frac{8\pi^2 \bar{D}_{11}}{\bar{C}} \\ u_0^{(1)} &= \mathcal{N} \sin(\pi x_1) \sin(\pi x_2), \quad u_0^{(2)} = \mathcal{N} \sin(2\pi x_1) \sin(\pi x_2), \\ u_0^{(3)} &= \mathcal{N} \sin(\pi x_1) \sin(2\pi x_2), \quad u_0^{(4)} = \mathcal{N} \sin(2\pi x_1) \sin(2\pi x_2) \end{aligned}$$

with the normalization constant $\mathcal{N} = 2/\sqrt{\bar{C}} \approx 0.26291$ since

$$(4.4) \quad \left(\int_0^1 \sin^2(m_1 \pi x_1) dx_1 \right) \cdots \left(\int_0^1 \sin^2(m_p \pi x_p) dx_p \right) = 2^{-p/2} \quad \forall \mathbf{m} \in \mathbb{N}^p.$$

We then solve the eigenvalue problem (4.2) using the Galerkin method with \mathbb{Q}_2 elements and a structured partition of both expanding directions into $12L$ intervals. According to Theorem 2.8, the non-relevant third direction is only discretized with six partitions since it is not relevant in the limit. Finally, we solve the corresponding algebraic eigenvalue problem using a block LOPCG method up to a tolerance of 10^{-6} .

For the error comparison, we project the analytical solutions (4.3) into the corresponding subspace \mathbb{H}_h . Since $\nu^{(2)} = \nu^{(3)}$ by our construction of ρ , the corresponding eigenspace is two-dimensional, and the eigensolver returns some basis of this space. To resolve these spatial rotations and allow for an error comparison, we align the second and third eigenfunction by modifying their discrete eigenvectors with

$$(4.5) \quad \mathbf{x}_h^{(2)} = \langle \mathbf{x}_h^{(2)}, \mathbf{x}_0^{(2)} \rangle \mathbf{x}_h^{(2)} + \langle \mathbf{x}_h^{(3)}, \mathbf{x}_0^{(2)} \rangle \mathbf{x}_h^{(3)}, \quad \mathbf{x}_h^{(3)} = \langle \mathbf{x}_h^{(2)}, \mathbf{x}_0^{(3)} \rangle \mathbf{x}_h^{(2)} + \langle \mathbf{x}_h^{(3)}, \mathbf{x}_0^{(3)} \rangle \mathbf{x}_h^{(3)},$$

where $\mathbf{x}_0^{(m)}$ denotes the m -th homogenized eigenvector. The resulting discrete eigenfunctions $u_{1/L,h}^{(m)}$ for $m = 1, 2, 3, 4$ are visualized in Figure 4 for $L \in \{2^0, \dots, 2^4\}$ together with the corresponding homogenized solutions $u_0^{(m)}$. We can observe that for larger domain lengths L , the eigenfunctions converge to their corresponding limits if we would neglect the oscillatory isolines that indicate strong gradients. This observation corresponds to our theoretical results that the convergence is only weak when considering the $H^1(\Omega_1)$ -norm. To quantify the convergence, we evaluate the relative $L^2(\Omega_1)$ -error of the eigenfunctions and the relative eigenvalue error in Figure 5 for $L \in \mathbb{R}$ with a sampling rate of $\Delta L = 0.1$. We measure a first-order convergence for the L^2 -error and at least first-order convergence for the eigenvalues. This observation matches the theoretical results from subsection 2.3 since we proved strong convergence in L^2 of the eigenfunctions and convergence of the eigenvalues to $\nu^{(m)}$. We also examine the eigenvalues and their ratios $\lambda_{1/L,h}^{(m)}/\lambda_{1/L,h}^{(m+1)}$ in Figure 5, where the degeneracy of $m = 2$, pre-asymptotic effects, and a non-monotonic convergence is visible. This observation confirms the prediction of Corollary 2.10 that the fundamental ratio can only be uniformly bounded for all $L > L^*$ when pre-asymptotic effects have vanished.

4.2. The Quasi-Optimal Shift-And-Invert Preconditioner. To show the practical advantage of using the quasi-optimal preconditioning technique of subsection 3.2, we compare the convergence histories of the IP and LOPCG method for

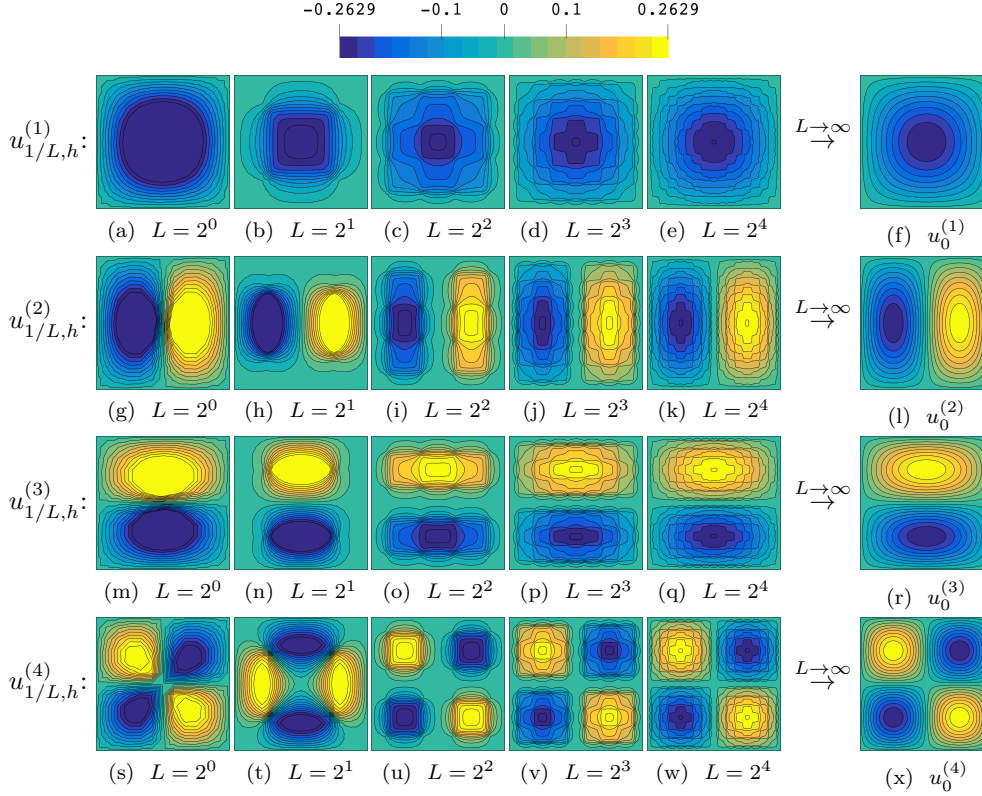


FIG. 4. The first four calculated eigenfunctions of the eigenvalue homogenization problem (4.2) converge weakly for $L \rightarrow \infty$ to the solutions of the homogenized equation. The figure presents two-dimensional cut-planes through the middle of the domain at $y_1 = 1/2$.

the cases of no shift ($\sigma = 0$), a good shift ($\sigma = 0.99\lambda_\infty$), and the quasi-optimal shift ($\sigma = \lambda_\infty$). We then aim to solve (1.2) on Ω_L for $\ell = 1$ and an increasing L . The quasi-optimal shift $\lambda_\infty = \lambda_{\mathcal{B}_\#, \mathcal{B}_d, 1, V}^{(1)}(\Omega_1)$ is obtained in constant time for all L since it only depends on the fixed unit cell Ω_1 . The calculations use \mathbb{Q}_1 finite elements on a regular mesh with mesh size $h = 1/100$ and the x -periodic potential $V(x, y) = 10^2 \sin(\pi x)^2 y^2$. We chose the start vectors $\mathbf{x}_0 = \mathbf{1}$, $\mathbf{x}_{-1} = \mathbf{e}_1$. The solvers aim to reduce the spectral residual $\mathbf{r}_k = \mathbf{A}\mathbf{x}_k - \mathbf{R}_{\mathbf{A}, \mathbf{B}}(\mathbf{x}_k)\mathbf{B}\mathbf{x}_k$ below the tolerance $\text{TOL} = 10^{-10}$ and stop after 100 iterations. Both algorithms converged to the lowest eigenpair since the shifting strategy is order-preserving (c.f. Remark 2.11), and the start vector \mathbf{x}_0 can not be orthogonal to the non-sign-changing ground state.

The results in Figure 6 indicate the drastic reduction in convergence speed for the unshifted algorithms. For the case of quasi-optimal preconditioning, both eigensolvers only need a couple of iterations to converge, as predicted by Theorem 2.9. When applying a good but not quasi-optimal shift of $0.99\lambda_\infty$, fast convergence rates for lower values of L can be observed. However, the convergence also deteriorates in the asymptotic limit of $L \rightarrow \infty$. This fact underlines the requirement for σ to be the exact asymptotic limit if the method shall provide convergence in a fixed number of iterations for all possible L . Furthermore, all three cases show a faster convergence of the LOPCG compared to the IP method.

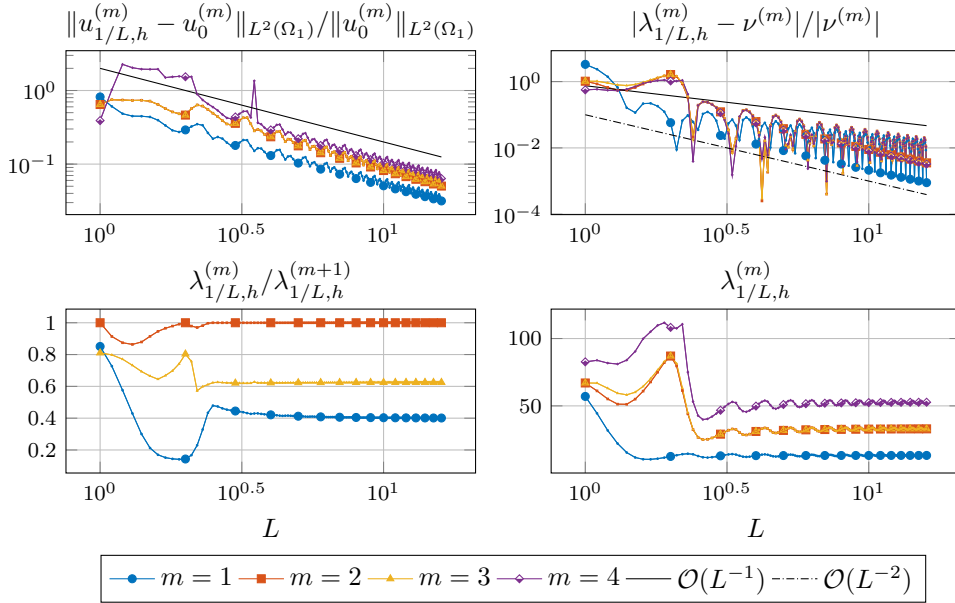


FIG. 5. Errors between the solution of (4.2) and the corresponding homogenized limit: We can observe the first-order convergence for all eigenfunctions in the L^2 -norm and at least first-order convergence for the eigenvalues. The ratios between two adjacent eigenvalues reveal a degenerate state and a non-monotonic convergence for the fundamental ratio $\lambda_{1/L,h}^{(1)}/\lambda_{1/L,h}^{(2)}$.

4.3. Extension to Complex Domains: Barrier Principle and Defects in x -Direction. The initial box setup of $\Omega_L = (0, L)^p \times (0, \ell)^q$ from section 1 is very suitable for the mathematical analysis performed in section 2. However, we need to generalize the theory to more realistic domains for practical applications. Luckily, this can be quite intuitively done with some simple considerations.

Consider, for example, the setup of Figure 7, in which one aims to simulate a union of three disks $\tilde{\Omega} = \bigcup_{i=1}^3 B_R((R + 2(i-1)r, 0)^T) = \tilde{\Omega}_{\text{left}} \cup \left(\bigcup_{i=1}^3 \tilde{\Omega}_i\right) \cup \tilde{\Omega}_{\text{right}}$ where $B_R(\mathbf{p})$ denotes a disk with radius R centered at \mathbf{p} and $r = R - d$ with the overlap d . These disks are all aligned along the x -axis and have a fixed overlap. We define the rectangular unit cell as the box with side lengths $\{2r, 2R\}$, where one disk is contained entirely. Inside this unit cell, we assume the potential as directional periodic. Furthermore, we have domain defects $\tilde{\Omega}_{\text{left}}$ and $\tilde{\Omega}_{\text{right}}$ that are not part of any unit cell on the left and the right side. In this setup, two problems arise – the simulation of non-box-shaped domains and the handling of domain defects.

4.3.1. Barrier Principle for an Optical Lattice Potential. We could simulate the whole domain $\Omega_{L=6r+2d}$ to overcome the first issue. However, we are only interested in the union-of-disks domain $\tilde{\Omega}$, and a prescription of Dirichlet values on $\partial\tilde{\Omega}$ might be problematic since it is inside the domain. It is well known that we can simply modify the potential V to achieve this setting. To avoid nontrivial values of ϕ_L in certain regions, we can apply a significant penalty term to V . We call this strategy the *barrier principle*, which extends a given potential V to the barrier potential $\tilde{V}(\mathbf{z}; V, a) = V(\mathbf{z}) + a\chi_{\tilde{\Omega}^c}(\mathbf{z})$ where $a \geq 0$ is a penalty term. $\chi_{\tilde{\Omega}^c}$ is the indicator function for the complement of $\tilde{\Omega}$. For an increasing value of $a \rightarrow \infty$, we can still

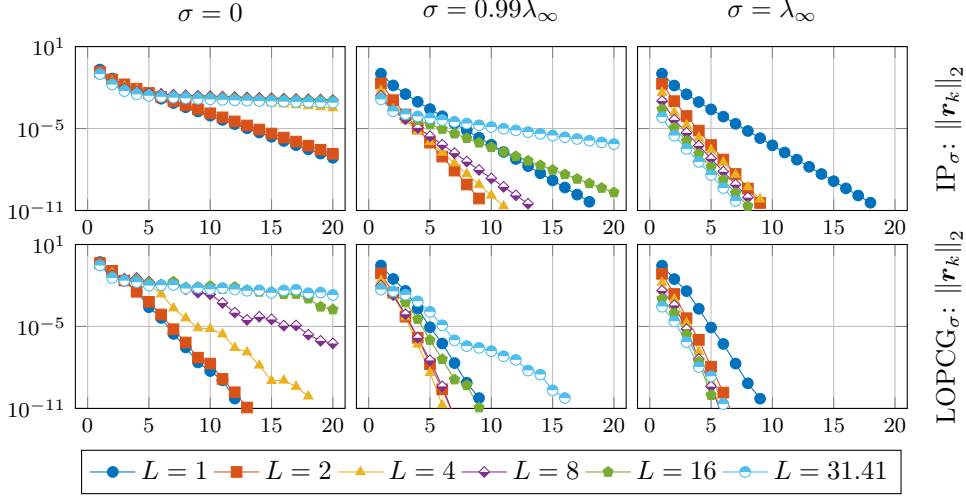


FIG. 6. A comparison of the IP_σ and $LOPCG_\sigma$ for the cases of $\sigma = 0$, $\sigma = 0.99\lambda_\infty$, and $\sigma = \lambda_\infty$ for different domain lengths L .

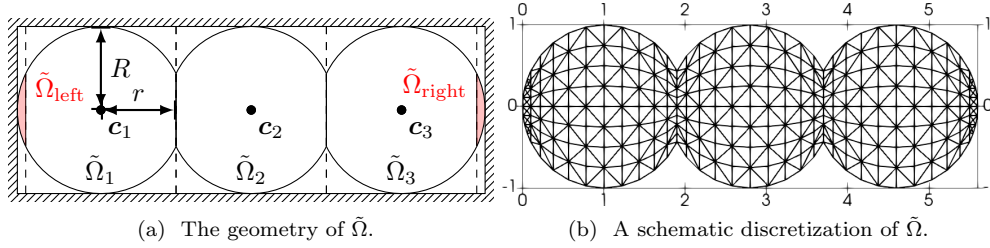


FIG. 7. A union of three disks ($R = 1$) domain with defects in the x -direction and overlap of $d = 0.1$: $\tilde{\Omega}$ comprises three identical unit cells $\tilde{\Omega}_i$ and two domain defects $\tilde{\Omega}_{left}, \tilde{\Omega}_{right}$.

apply our theory for any finite value of a . In the limit case, the eigenvalue problem on the box-shaped domain Ω_{6r+2d} is equivalent to an eigenvalue problem, purely posed on the subdomain $\tilde{\Omega} \subset \Omega_{6r+2d}$.

To demonstrate the barrier effect of $\tilde{V}(\mathbf{z}; V, a)$, we inspect the union of three disks case from [Figure 7](#) in combination with the optical lattice potential [\[42\]](#)

$$(4.6) \quad V(x, y) = 100 \left(1 - \sin \frac{\omega\pi(x-d)}{2(R-d)} \sin \frac{\omega\pi(y-(R-d))}{2(R-d)} \right),$$

where $\omega = 9, R = 1, d = 0.1$ for various penalty terms $a \in \{2^0, 2^5, \dots, 2^{20}\}$. [Figure 8](#) shows the first eigenfunction, which is calculated with the $LOPCG_{\sigma=0}$ method for $TOL = 10^{-10}$ on a structured \mathbb{Q}_1 -mesh with $h = 1/100$. It can be observed that with a increasing, the eigenfunction outside of $\tilde{\Omega}$ approaches zero. However, these above considerations are purely theoretical. In practice, we directly exclude the regions $\Omega_{6r+2d} \setminus \tilde{\Omega}$ and purely solve and mesh on $\tilde{\Omega}$ as displayed in [Figure 7b](#).

4.3.2. Principle of Defect Invariance. When it comes to simulating the domain of [subsection 4.3](#) with the quasi-optimally preconditioned eigensolver, we also need to calculate the shift $\sigma = \lambda_\infty$. For domains without any domain defect that perfectly match the potential's period, this is done by simulating one unit cell Ω_1 with

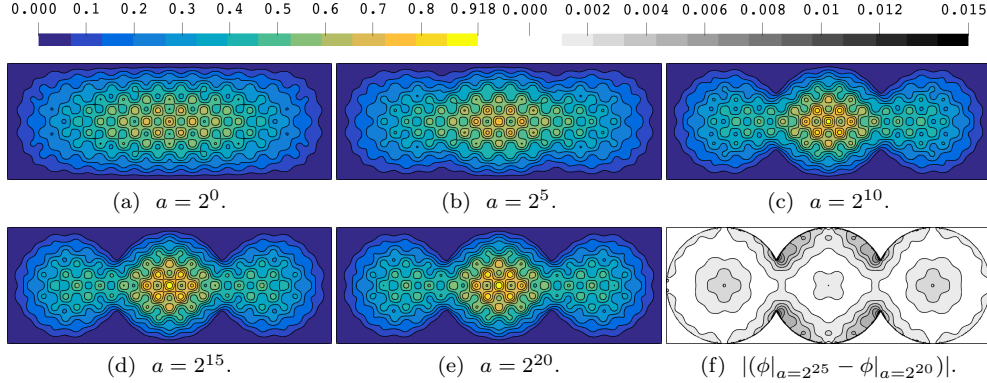


FIG. 8. Effect of Barrier Potential $\tilde{V}(\mathbf{z}; 0, a)$ for varying penalty parameters a in the union-of-disks domain $\tilde{\Omega}$ of Figure 7. With increasing a , the resulting problem statement reduces to the eigenproblem formulated in $\tilde{\Omega}$. When comparing the change between $a = 2^{15}$ and $a = 2^{20}$ in Figure 8f, the solution's overall change is small and focused on the connection points. Also, we see an interpolation error at the disk boundary since the underlying mesh is not boundary-aligned.

Dirichlet zero in \mathbf{y} - and periodic boundary conditions in \mathbf{x} -direction as theoretically derived in Theorems 2.5 and 2.8.

For the case of defects located at the extremities of the expanding \mathbf{x} -direction as a subset of an imaginary unit cell Ω_1 , we can do the same (if the potential acts as usual in the defect regions). The limit eigenvalue does not change since we can prove:

THEOREM 4.1 (Principle of Defect Invariance). *Let $\Omega_{L+2\delta}$ with L denoting the \mathbf{x} -period of the potential V and $\delta < L$ be given. For the linear Schrödinger eigenvalue problem (1.2) posed on $\Omega_{L+2\delta}$, it still holds that $\lim_{L \rightarrow \infty} \lambda_L^{(m)} = \lambda_{\varphi_y}$.*

Proof. Consider $\Omega_L \subset \Omega_{L+2\delta} \subset \Omega_{L+2}$. Then, by the inclusion principle [43, p13] for elliptic operators with Dirichlet boundary conditions, we have

$$(4.7) \quad \lambda_{\mathcal{B}_d, \mathcal{B}_d, 0, V}^{(m)}(\Omega_L) \leq \lambda_{\mathcal{B}_d, \mathcal{B}_d, 0, V}^{(m)}(\Omega_{L+2\delta}) \leq \lambda_{\mathcal{B}_d, \mathcal{B}_d, 0, V}^{(m)}(\Omega_{L+2})$$

Using the factorizations of Theorem 2.5, this is equivalent to

$$(4.8) \quad \lambda_{\varphi_y}^{(1)}(\Omega_L) + \lambda_{u_{y,2}}^{(m)}(\Omega_L) \leq \lambda_{\mathcal{B}_d, \mathcal{B}_d, 0, V}^{(m)}(\Omega_{L+2\delta}) \leq \lambda_{\varphi_y}^{(1)}(\Omega_{L+2}) + \lambda_{u_{y,2}}^{(m)}(\Omega_{L+2}).$$

Since $\lambda_{\varphi_y}^{(1)}(\Omega_L) = \lambda_{\varphi_y}^{(1)}(\Omega_{L+2}) = \lambda_{\varphi_y}^{(1)}(\Omega_1)$ and $\lambda_{u_{y,2}}^{(m)}(\Omega_L), \lambda_{u_{y,2}}^{(m)}(\Omega_{L+2}) \in \mathcal{O}(1/L^2)$ by Theorem 2.8, we conclude with the Sandwich Lemma. \square

We are now prepared to solve the union-of-disks geometry in the next subsection 4.4.

4.4. Chain Model with Truncated Coulomb Potential in Two Dimensions. Consider the domain $\tilde{\Omega}_N = \bigcup_{i=1}^N B_R \left((R + 2(i-1)r, 0)^T \right)$ with the parameters $R = 1, r = 0.9$. Chain-like molecules in the context of molecular simulations inspire this model. For real applications, the potential is a Coulomb potential. Since a singularity of V violates the assumption (A2), we use a truncated Coulomb potential as

$$(4.9) \quad V_{C, \text{lim}}(\mathbf{z}; b) = \begin{cases} -\frac{Z}{\|\mathbf{z}\|_2} & \text{for } \|\mathbf{z}\|_2 \geq b \\ -\frac{Z}{b} & \text{for } \|\mathbf{z}\|_2 < b \end{cases},$$

to mimic, e.g., the electrostatic potential with charge $Z > 0$. We also have to neglect long-range interaction to fulfill the periodicity assumption on V . Consider the N

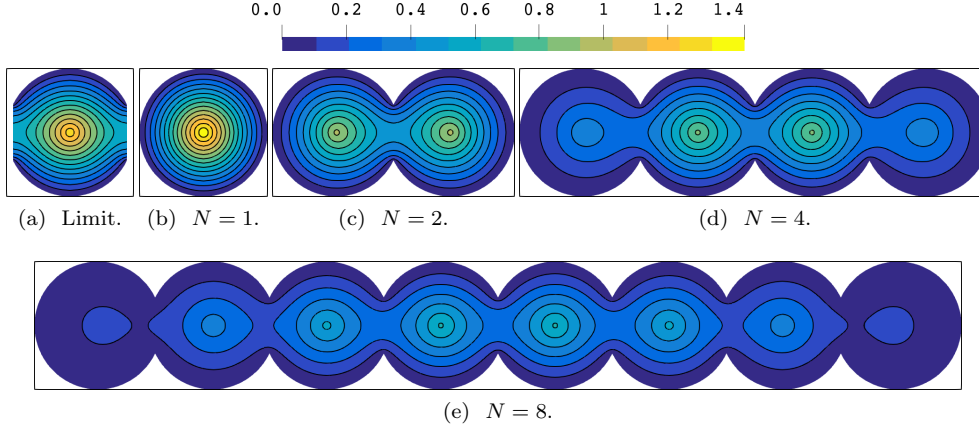


FIG. 9. Contours of the first eigenfunction for the union of N disks using the truncated Coulomb potential without long-range interactions: Figure 9a shows the asymptotic limit eigenfunction with periodic boundary conditions in the x -direction.

centers $\{\mathbf{c}_i\}_{i=1}^N$ with $\mathbf{c}_i = (R + (i-1)2r, 0)$. We prescribe the compound periodic potential $V(\mathbf{z}) = \sum_{i \in \{i: |\mathbf{z} - \tilde{\mathbf{c}}_i| < R\}} V_{C, \text{lim}}(\mathbf{z} - \tilde{\mathbf{c}}_i; b)$ where $\tilde{\mathbf{c}}_i \in \{\mathbf{c}_i\}_{i=1}^N \cup \{\mathbf{c}_1 - (2r, 0)\} \cup \{\mathbf{c}_N + (2r, 0)\}$ include ghost centers to fulfill the periodicity assumption (A1) also in the defect regions. We also note that the semi-positivity assumption (A3) is violated. However, it turned out that the resulting spectrum is still positive, the operator, thus, elliptic, and our theory is applicable. Nevertheless, it would also be possible to fulfill the assumption (A3) by adding a positive constant to the L^∞ -potential without changing the resulting eigenfunctions.

A series of computations for $N = 1, 2, 4, \dots, 32$ is performed using the LOPCG $_\sigma$ method for the potential parameters $Z = 1, b = 10^{-4}$ and the tolerance $\text{TOL} = 10^{-10}$. As shown in Figure 7b, the spatial discretization uses unstructured but symmetrically meshed \mathbb{P}_1 elements. The quasi-optimal shift calculation uses the unit cell $\tilde{\Omega}_0 = \tilde{\Omega}_1 \cap [R - r, R + r] \times [-R, R]$ with periodic boundary conditions in x -direction and zero boundary conditions on the rest. Thus, $\sigma = \lambda_{\varphi_y}(\tilde{\Omega}_0) \approx 1.08784$ can be computed a priori in $\mathcal{O}(1)$ since the unit cell is independent of N .

In Figure 9, the resulting ground state eigenfunctions $\phi_h^{(1)}$ are presented with the solution to the base problem in Figure 9a. We can observe for increasing N that the solution inside a single disk approaches the shape of the solution to the unit cell problem. This convergence is the expected behavior, as shown theoretically in section 2. In Table 1, we observe that, due to the quasi-optimal preconditioning, the number of iterations needed to meet the required residual tolerance is of order $\mathcal{O}(1)$. Furthermore, the method shows a linearly scaling behavior since the ratio of calculation time to the disk amount t_{eig}/N seems to be independent of N .

4.5. Plane Model with Kronig–Penney Potential in Three Dimensions.

Finally, we also show the preconditioner's quasi-optimality for a three-dimensional case with two expanding directions ($p = 2, q = 1$). We use a three-dimensional Kronig–Penney potential [58], defined by $V(\mathbf{z}) = 0$ for $\|\mathbf{z} \bmod \mathbf{1} - \mathbf{1}/2\|_1 < 1/4$ and $V(\mathbf{z}) = 100$ otherwise, where $\mathbf{1}$ denotes the vector of ones in d dimensions. This potential represents cubic wells with sidelength 0.5 centered in the unit cubes, which form the plane-like expanding domain $\Omega_L = (0, L)^2 \times (0, 1)$ with $L \in \mathbb{N}$. We again calculate the quasi-optimal shift $\sigma = \lambda_{\mathcal{B}_{\#}, \mathcal{B}_{d,1}, V}^{(1)}(\Omega_1)$ on the unit cube and use it to

TABLE 1

The summary of computations for the union of N disks with the truncated Coulomb potential. Due to the same discretization density, the number of nodes n_{nodes} for each mesh is approximately proportional to the number of disks N (up to the defects). The wall times are measured on an Intel X7542 CPU using one core.

$N \propto L$	n_{nodes}	$\lambda_h^{(1)}$	$\max \phi_h^{(1)}$	k_{it}	$\frac{\lambda_{\max}(A-\sigma B)}{\lambda_{\min}(A-\sigma B)}$	$t_{\text{eig}} [s]$	$\frac{t_{\text{eig}}}{N} [s]$
1	89,869	1.96222	1.44	5	$4.83 \cdot 10^5$	1.83	1.83
2	$1.69 \cdot 10^5$	1.46912	0.96	5	$1.25 \cdot 10^6$	3.95	1.97
4	$3.27 \cdot 10^5$	1.20013	0.85	5	$4.25 \cdot 10^6$	7.7	1.92
8	$6.44 \cdot 10^5$	1.11768	0.64	5	$1.14 \cdot 10^7$	17.03	2.13
16	$1.28 \cdot 10^6$	1.0955	0.46	5	$2.55 \cdot 10^7$	33.06	2.07
32	$2.54 \cdot 10^6$	1.08978	0.33	5	$5.33 \cdot 10^7$	64.96	2.03

TABLE 2

The summary of computations for the plane-like expanding domain in three directions with the Kronig-Penney potential. The number of unit cells N now scales quadratically with L .

L	n_{nodes}	$\lambda_h^{(1)}$	$\max \phi_h^{(1)}$	k_{it}	$t_{\text{eig}} [s]$	$\frac{t_{\text{eig}}}{L^2} [s]$
1	1,331	58.99915	4.71	5	0.16	0.16
2	4,851	58.30881	2.31	6	0.52	0.13
4	18,491	57.81186	1.95	6	3.01	0.19
8	72,171	57.6587	1.09	7	15.28	0.24
16	$2.85 \cdot 10^5$	57.61845	0.56	7	73.33	0.29
32	$1.13 \cdot 10^6$	57.60826	0.28	6	320.64	0.31

precondition the Ω_L -problem. Finally, both problems are discretized using a uniform mesh size of $h = 1/10$ and \mathbb{Q}_1 elements resulting in $\sigma \approx 57.60485$. We use the LOPCG $_{\sigma}$ method with $\text{TOL} = 10^{-10}$ and solve for the ground state solution. The simulations are performed on a series of domains Ω_L with $L \in \{1, 2, 4, \dots, 32\}$. In Table 2, we observe that the number of eigensolver iterations k_{it} does not increase for $L \rightarrow \infty$, confirming our theory. However, in contrast to Table 1, a slight increase in solution time per number of unit cells (t_{eig}/L^2) can be observed. This increase is the expected behavior of using a direct solver for sparse matrices with increased bandwidth for $L \rightarrow \infty$ for our case of $p = 2$ expanding directions.

5. Conclusion. This work presented a quasi-optimal shift-and-invert preconditioner to solve the linear periodic Schrödinger eigenvalue problem in a constant number of eigensolver iterations for domains expanding periodically in a subset of directions. First, we analyzed and proved the quasi-optimality of the method using factorization and homogenization techniques. The analysis revealed powerful insights into the behavior of the eigenfunctions and eigenvalues. Significantly, the representation of the searched eigenfunction as the product of easy-to-calculate functions leads to a decisive result – the corresponding eigenvalues can be expressed as the sum of other eigenvalues, which can be much easier computed in practice than solving the whole system. This realization makes the proposed method very practical since calculating the quasi-optimal shift can be done in $\mathcal{O}(1)$. We then extended the results to complex and defect domain shapes to allow for a broader range of geometrical applications. Finally, in our experiments, we showed the practical usability of the method for chain-like and plane-like expanding domains.

Limitations of our method include the assumptions on the potential V to be

essentially bounded and periodic. Also, we observed that using the perfect shift in the eigensolver algorithms leads naturally to an ill-conditioned system matrix $(\mathbf{A} - \sigma\mathbf{B})$. Thus, future work could weaken the periodicity assumptions on V by, e.g., allowing for a perturbation of δV that vanishes in the limit $L \rightarrow \infty$. Also, efficient solvers for the linear system involving $(\mathbf{A} - \sigma\mathbf{B})$ must be constructed when the system size requires iterative linear solvers.

REFERENCES

- [1] P. M. AJAYAN AND O. Z. ZHOU, *Applications of Carbon Nanotubes*, in Carbon Nanotubes: Synthesis, Structure, Properties, and Applications, M. S. Dresselhaus, G. Dresselhaus, and P. Avouris, eds., Topics in Applied Physics, Springer, Berlin, Heidelberg, 2001, pp. 391–425, https://doi.org/10.1007/3-540-39947-X_14.
- [2] G. ALLAIRE, *Numerical Analysis and Optimization: An Introduction to Mathematical Modelling and Numerical Simulation*, Numerical Mathematics and Scientific Computation, Oxford University Press, 2007.
- [3] G. ALLAIRE, *A brief introduction to homogenization and miscellaneous applications*, ESAIM: Proceedings, 37 (2012), pp. 1–49, <https://doi.org/10.1051/proc/201237001>.
- [4] G. ALLAIRE AND G. BAL, *Homogenization of the criticality spectral equation in neutron transport*, ESAIM: Mathematical Modelling and Numerical Analysis, 33 (1999), pp. 721–746, <https://doi.org/10.1051/m2an:1999160>.
- [5] G. ALLAIRE AND Y. CAPDEBOSCQ, *Homogenization of a spectral problem in neutronic multi-group diffusion*, Computer Methods in Applied Mechanics and Engineering, 187 (2000), pp. 91–117, [https://doi.org/10.1016/S0045-7825\(99\)00112-7](https://doi.org/10.1016/S0045-7825(99)00112-7).
- [6] G. ALLAIRE AND Y. CAPDEBOSCQ, *Homogenization and localization for a 1-D eigenvalue problem in a periodic medium with an interface*, Annali di Matematica Pura ed Applicata, 181 (2002), pp. 247–282, <https://doi.org/10.1007/s102310100040>.
- [7] G. ALLAIRE AND C. CONCA, *Bloch wave homogenization and spectral asymptotic analysis*, Journal de Mathématiques Pures et Appliquées, 77 (1998), pp. 153–208, [https://doi.org/10.1016/S0021-7824\(98\)80068-8](https://doi.org/10.1016/S0021-7824(98)80068-8).
- [8] G. ALLAIRE AND F. MALIGE, *Analyse asymptotique spectrale d'un problème de diffusion neutronique*, Comptes Rendus de l'Académie des Sciences - Series I - Mathematics, 324 (1997), pp. 939–944, [https://doi.org/10.1016/S0764-4442\(97\)86972-8](https://doi.org/10.1016/S0764-4442(97)86972-8).
- [9] G. ALLAIRE AND A. PIATNITSKI, *Homogenization of the Schrödinger Equation and Effective Mass Theorems*, Communications in Mathematical Physics, 258 (2005), pp. 1–22, <https://doi.org/10.1007/s00220-005-1329-2>.
- [10] M. ALNÆS, J. BLECHTA, J. HAKE, A. JOHANSSON, B. KEHLET, A. LOGG, C. RICHARDSON, J. RING, M. E. ROGNES, AND G. N. WELLS, *The FEniCS Project Version 1.5*, Archive of Numerical Software, 3 (2015), <https://doi.org/10.11588/ans.2015.100.20553>.
- [11] R. ALTMANN, P. HENNING, AND D. PETERSEIM, *Quantitative Anderson localization of Schrödinger eigenstates under disorder potentials*, Mathematical Models and Methods in Applied Sciences, 30 (2020), pp. 917–955, <https://doi.org/10.1142/S0218202520500190>.
- [12] R. ALTMANN, P. HENNING, AND D. PETERSEIM, *The J-method for the Gross–Pitaevskii eigenvalue problem*, Numerische Mathematik, 148 (2021), pp. 575–610, <https://doi.org/10.1007/s00211-021-01216-5>.
- [13] R. ALTMANN, P. HENNING, AND D. PETERSEIM, *Localization and Delocalization of Ground States of Bose–Einstein Condensates Under Disorder*, SIAM Journal on Applied Mathematics, 82 (2022), pp. 330–358, <https://doi.org/10.1137/20M1342434>.
- [14] R. ALTMANN AND D. PETERSEIM, *Localized Computation of Eigenstates of Random Schrödinger Operators*, SIAM Journal on Scientific Computing, 41 (2019), pp. B1211–B1227, <https://doi.org/10.1137/19M1252594>.
- [15] X. ANTOINE AND R. DUBOSCQ, *GPELab, a Matlab toolbox to solve Gross–Pitaevskii equations I: Computation of stationary solutions*, Computer Physics Communications, 185 (2014), pp. 2969–2991, <https://doi.org/10.1016/j.cpc.2014.06.026>.
- [16] X. ANTOINE AND R. DUBOSCQ, *GPELab, a Matlab toolbox to solve Gross–Pitaevskii equations II: Dynamics and stochastic simulations*, Computer Physics Communications, 193 (2015), pp. 95–117, <https://doi.org/10.1016/j.cpc.2015.03.012>.
- [17] X. ANTOINE, A. LEVITT, AND Q. TANG, *Efficient spectral computation of the stationary states of rotating Bose–Einstein condensates by the preconditioned nonlinear conjugate gradient method*, Journal of Computational Physics, 343 (2017), pp. 92–109, <https://doi.org/10.1016/j.jcp.2017.03.012>.

- 1016/j.jcp.2017.04.040.
- [18] I. BABUŠKA AND J. E. OSBORN, *Finite Element-Galerkin Approximation of the Eigenvalues and Eigenvectors of Selfadjoint Problems*, Mathematics of Computation, 52 (1989), p. 24.
 - [19] S. BADIA AND F. VERDUGO, *Gridap: An extensible Finite Element toolbox in Julia*, Journal of Open Source Software, 5 (2020), p. 2520, <https://doi.org/10.21105/joss.02520>.
 - [20] Z. BAI, J. DEMMEL, J. DONGARRA, A. RUHE, AND H. VAN DER VORST, eds., *Templates for the Solution of Algebraic Eigenvalue Problems: A Practical Guide*, Society for Industrial and Applied Mathematics, Jan. 2000, <https://doi.org/10.1137/1.9780898719581>.
 - [21] J. BEZANSON, A. EDELMAN, S. KARPINSKI, AND V. B. SHAH, *Julia: A Fresh Approach to Numerical Computing*, SIAM Review, 59 (2017), pp. 65–98, <https://doi.org/10.1137/141000671>.
 - [22] H. BREZIS, *Functional Analysis, Sobolev Spaces and Partial Differential Equations*, Springer New York, New York, NY, 2010, <https://doi.org/10.1007/978-0-387-70914-7>.
 - [23] E. CANCÈS, L. GARRIGUE, AND D. GONTIER, *Second-order homogenization of periodic Schrödinger operators with highly oscillating potentials*, 2021, <https://arxiv.org/abs/2112.12008>.
 - [24] E. CANCÈS, G. KEMLIN, AND A. LEVITT, *Convergence Analysis of Direct Minimization and Self-Consistent Iterations*, SIAM Journal on Matrix Analysis and Applications, 42 (2021), pp. 243–274, <https://doi.org/10.1137/20M1332864>.
 - [25] S. CARR, D. MASSATT, S. B. TORRISI, P. CAZEAUX, M. LUSKIN, AND E. KAXIRAS, *Relaxation and domain formation in incommensurate two-dimensional heterostructures*, Physical Review B, 98 (2018), pp. 224102–1–224102–7, <https://doi.org/10.1103/PhysRevB.98.224102>.
 - [26] P. CAZEAUX, M. LUSKIN, AND D. MASSATT, *Energy Minimization of Two Dimensional Incommensurate Heterostructures*, Archive for Rational Mechanics and Analysis, 235 (2020), pp. 1289–1325, <https://doi.org/10.1007/s00205-019-01444-y>.
 - [27] M. CHIPOT, *On some anisotropic singular perturbation problems*, Asymptotic Analysis, (2007), p. 21, <https://doi.org/10.5167/uzh-21524>.
 - [28] M. CHIPOT, *L goes to plus infinity: An update*, Journal of the Korean Society for Industrial and Applied Mathematics, 18 (2014), pp. 107–127, <https://doi.org/10.12941/JKSIAM.2014.18.107>.
 - [29] M. CHIPOT, A. ELFANNI, AND A. ROUGIREL, *Eigenvalues, Eigenfunctions in Domains Becoming Unbounded*, in Hyperbolic Problems and Regularity Questions, M. Padula and L. Zanghirati, eds., Birkhäuser Basel, Basel, 2007, pp. 69–78, https://doi.org/10.1007/978-3-7643-7451-8_8.
 - [30] M. CHIPOT, W. HACKBUSCH, S. SAUTER, AND A. VEIT, *Numerical Approximation of Poisson Problems in Long Domains*, Vietnam Journal of Mathematics, (2021), <https://doi.org/10.1007/s10013-021-00512-9>.
 - [31] M. CHIPOT AND A. ROUGIREL, *On the asymptotic behaviour of the solution of elliptic problems in cylindrical domains becoming unbounded*, Communications in Contemporary Mathematics, 04 (2002), pp. 15–44, <https://doi.org/10.1142/S0219199702000555>.
 - [32] M. CHIPOT AND A. ROUGIREL, *On the asymptotic behaviour of the eigenmodes for elliptic problems in domains becoming unbounded*, Transactions of the American Mathematical Society, 360 (2008), pp. 3579–3603, <https://doi.org/10.1090/S0002-9947-08-04361-4>.
 - [33] M. CHIPOT, P. ROY, AND I. SHAFRIR, *Asymptotics of eigenstates of elliptic problems with mixed boundary data on domains tending to infinity*, Asymptotic Analysis, 85 (2013), pp. 199–227, <https://doi.org/10.3233/ASY-131182>.
 - [34] M. CHIPOT AND Y. XIE, *On the asymptotic behaviour of elliptic problems with periodic data*, Comptes Rendus Mathématique, 339 (2004), pp. 477–482, <https://doi.org/10.1016/j.crma.2004.09.007>.
 - [35] R. COURANT AND D. HILBERT, *Methods of Mathematical Physics. Volume I*, Wiley, New York, 1989, <https://doi.org/10.1002/9783527617210>.
 - [36] R. DONG, D. LI, AND L. WANG, *Regularity of elliptic systems in divergence form with directional homogenization*, Discrete & Continuous Dynamical Systems - A, 38 (2018), pp. 75–90, <https://doi.org/10.3934/dcds.2018004>.
 - [37] R. DONG, D. LI, AND L. WANG, *Directional homogenization of elliptic equations in non-divergence form*, Journal of Differential Equations, 268 (2020), pp. 6611–6645, <https://doi.org/10.1016/j.jde.2019.11.041>.
 - [38] M. A. FREITAG AND A. SPENCE, *Convergence of inexact inverse iteration with application to preconditioned iterative solves*, BIT Numerical Mathematics, 47 (2007), pp. 27–44, <https://doi.org/10.1007/s10543-006-0100-1>.
 - [39] M. GALEWSKI, B. GALEWSKA, AND E. SCHMEIDEL, *Conditions for having a diffeomorphism between two Banach spaces*, Electronic Journal of Differential Equations, 99 (2014), pp. 1–

- 6.
- [40] D. GILBARG AND N. S. TRUDINGER, *Elliptic Partial Differential Equations of Second Order*, Classics in Mathematics, Springer-Verlag, Berlin Heidelberg, second ed., 2001, <https://doi.org/10.1007/978-3-642-61798-0>.
 - [41] P. HEID, B. STAMM, AND T. P. WIHLER, *Gradient flow finite element discretizations with energy-based adaptivity for the Gross-Pitaevskii equation*, Journal of Computational Physics, 436 (2021), p. 110165, <https://doi.org/10.1016/j.jcp.2021.110165>.
 - [42] P. HENNING AND D. PETERSEIM, *Sobolev Gradient Flow for the Gross–Pitaevskii Eigenvalue Problem: Global Convergence and Computational Efficiency*, SIAM Journal on Numerical Analysis, 58 (2020), pp. 1744–1772, <https://doi.org/10.1137/18M1230463>.
 - [43] A. HENROT, *Extremum Problems for Eigenvalues of Elliptic Operators*, Frontiers in Mathematics, Birkhäuser Basel, 2006, <https://doi.org/10.1007/3-7643-7706-2>.
 - [44] M. F. HERBST AND A. LEVITT, *Black-box inhomogeneous preconditioning for self-consistent field iterations in density functional theory*, Journal of Physics: Condensed Matter, 33 (2021), p. 085503, <https://doi.org/10.1088/1361-648X/abcdbd>.
 - [45] V. V. JIKOV, S. M. KOZLOV, AND O. A. OLEINIK, *Homogenization of Differential Operators and Integral Functionals*, Springer-Verlag, Berlin Heidelberg, 1994, <https://doi.org/10.1007/978-3-642-84659-5>.
 - [46] S. KESAVAN, *Homogenization of elliptic eigenvalue problems: Part 1*, Applied Mathematics and Optimization, 5 (1979), pp. 153–167, <https://doi.org/10.1007/BF01442551>.
 - [47] S. KESAVAN, *Homogenization of elliptic eigenvalue problems: Part 2*, Applied Mathematics and Optimization, 5 (1979), pp. 197–216, <https://doi.org/10.1007/BF01442554>.
 - [48] A. KUTNER AND A.-M. SÄNDIG, *Some Applications of Weighted Sobolev Spaces*, vol. 100 of Teubner-Texte Zur Mathematik, Vieweg+Teubner Verlag, Wiesbaden, 1987, <https://doi.org/10.1007/978-3-663-11385-0>.
 - [49] S. LEONARDI, *The best constant in weighted Poincaré and Friedrichs inequalities*, Rendiconti del Seminario Matematico della Università di Padova, 92 (1994), pp. 195–208.
 - [50] G. PAPANICOLAU, A. BENSOUSSAN, AND J.-L. LIONS, *Asymptotic Analysis for Periodic Structures, Volume 5 - 1st Edition*, North Holland, 1978.
 - [51] Y. SAAD, *Numerical Methods for Large Eigenvalue Problems*, no. 66 in Classics in Applied Mathematics, Society for Industrial and Applied Mathematics, Philadelphia, 2011, <https://doi.org/10.1137/1.9781611970739>.
 - [52] F. SANTOSA AND M. VOGELIUS, *First-Order Corrections to the Homogenized Eigenvalues of a Periodic Composite Medium*, SIAM Journal on Applied Mathematics, 53 (1993), pp. 1636–1668, <https://doi.org/10.1137/0153076>.
 - [53] J. SUN AND A. ZHOU, *Finite Element Methods for Eigenvalue Problems*, Chapman and Hall/CRC, 2016, <https://doi.org/10.1201/9781315372419>.
 - [54] T. A. SUSLINA, *On homogenization for a periodic elliptic operator in a strip*, St. Petersburg Math. J., 16 (2004), pp. 237–258, <https://doi.org/10.1090/S1061-0022-04-00849-0>.
 - [55] L. THEISEN AND B. STAMM, *ddEigenLab.jl: Domain-Decomposition Eigenvalue Problem Lab*. Zenodo, May 2022, <https://doi.org/10.5281/zenodo.6576197>.
 - [56] L. THEISEN AND M. TORRILHON, *fenicsR13: A Tensorial Mixed Finite Element Solver for the Linear R13 Equations Using the FEniCS Computing Platform*, ACM Transactions on Mathematical Software, 47 (2021), pp. 17:1–17:29, <https://doi.org/10.1145/3442378>.
 - [57] M. VANNINATHAN, *Homogenization of eigenvalue problems in perforated domains*, Proceedings of the Indian Academy of Sciences - Section A, 90 (1981), pp. 239–271, <https://doi.org/10.1007/BF02838079>.
 - [58] K. VARGA AND J. A. DRISCOLL, *Computational Nanoscience: Applications for Molecules, Clusters, and Solids*, Cambridge University Press, Cambridge, 2011, <https://doi.org/10.1017/CBO9780511736230>.
 - [59] K. B. VU, V. V. VU, H. P. THI THU, H. N. GIANG, N. M. TAM, AND S. T. NGO, *Conjugated polymers: A systematic investigation of their electronic and geometric properties using density functional theory and semi-empirical methods*, Synthetic Metals, 246 (2018), pp. 128–136, <https://doi.org/10.1016/j.synthmet.2018.10.007>.
 - [60] Y. ZHANG, *Estimates of eigenvalues and eigenfunctions in elliptic homogenization with rapidly oscillating potentials*, Journal of Differential Equations, 292 (2021), pp. 388–415, <https://doi.org/10.1016/j.jde.2021.05.006>.
 - [61] V. V. ZHIKOV, *Weighted Sobolev spaces*, Sbornik: Mathematics, 189 (1998), pp. 1139–1170, <https://doi.org/10.1070/SM1998v189n08ABEH000344>.